TECHNISCHE UNIVERSITÄT WIEN

VIENNA UNIVERSITY OF TECHNOLOGY

Diplomarbeit

Propagation of High Power Laser Pulses through Photonic Band Gap Fiber

Ausgeführt zum Zwecke des Erlangens des akademischen Grades eines Diplomingenieurs

unter der Leitung von

A. o. Univ. Prof. Univ. Prof. Dr. phil. Ernst WINTNER
Institut für Photonik

mit Unterstützung von

Dipl.-Ing. Heinrich KOFLER
Institut für Photonik

Durchgeführt am
Institut für Photonik der Technischen Universität Wien

Eingereicht an der Technischen Universität Wien
Fakultät für Elektrotechnik

von

Filip ORBAN
Matr. Nr. 9825101
Zehnergasse 20/A/27
2700 Wiener Neustadt

Wien, im Mai 2006

Abstract

The subject of this work deals with the transmission of high power nanosecond laser pulses through a single-mode hollow core photonic band gap fiber. Tests of potential applications have shown that pulses of some nanoseconds length are the best solution for laser ignition of engines. For the performed experiments Q-switched Nd:YAG lasers were used, which produced short pulses of 6 and 10 ns duration, maximum pulse energies of up to 400 mJ per pulse and repetition rates from 2 to 12.5 pulses per second at a wavelength of 1064 nm.

The purpose of this work was to find out if it is possible to use photonic crystal fibers for laser ignition. It has been figured out earlier, that conventional mono-mode glass fiber cannot deliver optical pulses of high enough power, without exceeding their damage threshold, in order to ignite a gas mixture as it is employed in internal combustion engines. Additionally the energy output/input efficiency should be discovered.

Many aspects had to be examined to show that photonic band gap fibers provide a reliable medium for transmission of such laser pulses. One of the most important and fundamental aspects was to couple the laser beam perfectly into the hollow core of the fiber. Visualisation of the coupling process was performed with the help of a CCD camera. When the laser beam was perfectly adjusted to the middle of the core and thus transmitting most of the laser power with minimum attenuation, the coupling was successfully accomplished. It is important to mention that in practical experiments coupling efficiency of 82 % was achieved. Only after the coupling procedure, other aspects could be considered, such as a demonstration of non-destructive transmission of laser pulses exceeding the power density level of plasma formation in air. To overcome this threshold intensity, which lies at around 200 GW/cm^2 and immediately would result

in the damage of the fiber material, a vacuum chamber has been established to offer the possibility to evacuate the hollow core.

The breakdown thresholds in the gradually evacuated core were measured to find out the required energy levels depending on a systematic change in pressure. Under certain experimental conditions was observed, that the lower the pressure was established, the higher the energy of pulses could be applied for transmission. Beside the afore mentioned evacuation, the ability to propagate only the fundamental mode makes this fiber the ideal transmission medium for high power laser pulses, because the laser beam coming out of the fiber has to be refocused into a gas chamber. Such tight focusing can be performed only with a high quality beam. Former experiments demonstrated additionally, that through a standard monomode optical fiber sufficient energy cannot be passed to form plasma for ignition of the gas in the chamber. In contrast, the conventional multi-mode optical fiber cannot be used either, due to the impossibility of focusing the beam after the fiber so that plasma can be formed in the gas chamber.

The aim was to provide stable and reliable guiding of high power laser pulses for long time without the fiber suffering any kind of damage, which was partially achieved. Despite the evacuation, the maximum energy received at the output of the fiber was 780 μJ in the case of 10 ns pulse duration and 200 μJ in the case of 6 ns pulse duration.

Kurzfassung

Diese Arbeit beschäftigte sich mit der Übertragung von Hochleistungslaserimpulsen durch eine mono-modige photonische Faser mit einem hohlen Kern. Die zwecks potentieller Anwendungen durchgeführten Tests haben gezeigt, dass Laserimpulse mit wenigen ns Dauer für die Laserzündung besonders geeignet sind. Für die im Rahmen dieser Diplomarbeit durchgeführten Experimente wurden aktiv güte-geschaltete Nd:YAG Laser verwendet, die Impulse mit einer maximalen Pulsenergie von 400 mJ und mit einer Pulsdauer von 6 und 10 ns bei einer Repetitionsrate von 2 bis 12.5 Hz und einer Wellenlänge von 1064 nm produzierten.

Das Ziel der Arbeit war es herauszufinden, ob es günstig ist, photonische Fasern für die Laserzündung einzusetzen. Man hat schon früher herausgefunden, dass die konventionellen single-modigen optischen Fasern nicht fähig waren, Laserimpulse mit einer Spitzenleistung zu übertragen, die notwendig gewesen wäre, um Gasmischungen in einem Verbrennungsraum zu entzünden. Zusätzlich sollte auch die Energieeffizienz der Ausgangsenergie zu Eingangsenergie untersucht werden.

Verschiedene Aspekte mussten überprüft werden, um die photonische Faser als zuverlässiges Übertragungsmedium von Hochleistungslaserimpulsen in Betracht ziehen zu können. Der wichtigste Aspekt war die perfekte Einkopplung der Laserstrahlen in den Faserkern, die mit Hilfe einer CCD Kamera kontrolliert wurde. Der Einkopplungsprozess wurde als erfolgreich angesehen, wenn der Laserstrahl in die Mitte des Kerns eingestellt und so die höchstmögliche Leistung mit der niedrigsten Abschwächung übertragen wurde. Auf diese Art und Weise wurde eine Effizienz von 82 % erreicht. Erst nach der erfolgreichen Einkopplung konnten andere Aspekte ermittelt werden, wie zum Beispiel die Untersuchung der Zerstörschwellen während der Übertragung. Um eine zerstörungsfreie Über-

tragung der Laserimpulse, die den Grenzwert der Plasmabildung in der Luft bei einer Intensität von 200 GW/cm^2 überschritten haben, garantieren zu können, wurde eine Vakuumkammer eingerichtet, damit der hohle Kern der photonischen Faser evakuiert werden konnte.

Die Zerstörschwellen der stufenweise evakuierten photonischen Faser wurden gemessen, damit beurteilt werden konnte, ob es einen Zusammenhang zwischen dem herrschenden Druck in der Vakuumkammer und der Energieschwelle gäbe. Die Fähigkeit der photonischen Faser nur die Grundmode zu übertragen, macht diese Faser besonders für die Laserzündung interessant, weil der Laserstrahl nach der erfolgreichen Übertragung wieder in die Verbrennungskammer fokusiert werden muss. Diese Refokussierung des Strahles funktioniert am besten mit einem Laserstrahl, der nur die Grundmode enthält. Das zeigte sich auch in früheren Untersuchungen von multi-modigen Stufenindexfasern mit einem grossen Kerndurchmesser, deren multi-modiger Strahl unter eine bestimmte Grösse nicht fokussiert werden konnte, um Gasgemische zünden zu können, obwohl die Impulsenergie dafür ausgereicht hätte.

Das Wunschziel war eine stabile und zuverlässige Übertragung von Hochleistungslaserimpulsen für eine sehr lange Dauer, ohne irgendeine Art Zerstörung der Faser zu erleiden, das in einem einschränkenden Teil auch erreicht wurde. Trotz einer Evakuierung wurde eine maximale Ausgansenergie von 780 μJ im Falle einer 10 ns Impulsdauer und 200 μJ im Falle einer 6 ns Impulsdauer gemessen.

Acknowledgements

I would like to give a special thank to Prof. Dr. Ernst Wintner (Photonics Institute) for the offer and the supervision of my work on the latest and very interesting topic. For the great support I want to appreciate Prof. Dr. Georg Reider, Dipl.-Ing. Heinrich Kofler and Dr. Martin Weinrotter.

Special thank goes also to the members of the International Laser Center in Moscow, to Prof. Dr. Aleksey M. Zheltikov, Dr. Dmitri A. Sidorov-Biryukov and Dr. Andrey B. Fedotov for making it possible for me to get an interesting and instructive experience in the laboratory of the Chair of General Physics and Wave Processes at the Lomonosov Moscow State University within the scope of an exchange project financially supported by ÖAD (Austrian Academic Exchange Service). Inside and outside of the laboratory I got a great support from the students: Vladimir P. Mitrokhin, Ilya V. Fedotov and Ulyana I. Alekseyeva.

For the perfect images of the PBG fiber made by the environmental scanning electron microscope I would like to thank Prof. Dr. Johann Wernisch from Institute of Solid State Physics.

The glass cupola for the vacuum chamber was kindly provided by Dr. Franz Keplinger from the Institute of Sensor and Actuator Systems.

Finally, I would like thank my family for the limitless support.

Contents

1. Propagation principles for optical fibers **1**

1.1. Total internal reflection 1

1.2. Multiple reflections 2

1.3. Gaussian beam definition 4

1.4. Quality of the laser beam and M^2 7

1.4.1. "Second moment" method for determining of M^2 8

1.4.2. Scanning slit method for determinination of M^2 11

1.4.3. Pinhole method for determinination of M^2 12

1.4.4. Knife edge method for determinination of M^2 12

1.4.5. CCD - Charge Coupled Device used for determination of M^2 . . . 13

2. Experiments **14**

2.1. Experimental setup 15

2.2. Alignment 19

2.2.1. Adjustable microscope objectives and fixed fiber 21

2.2.2. Fixed lenses and adjustable fiber 22

2.3. Selection of focusing lenses 22

2.4. Cleaving 25

2.4.1. Procedure of cleaving 26

2.4.2. Examination of the cleaving result 28

2.5. Coupling 29

2.5.1. Procedure for coupling 30

2.5.2. Interpretation of recorded images related to coupling procedure . 31

2.6. Evacuation of the vacuum chamber 32

3. Results **35**

3.1. Transmission spectrum of the PBG fiber 35

3.2. M^2 of the employed lasers 36

3.2.1. Quantel Brilliant 38

3.2.2. Litron 39

3.2.3. Summary 41

3.3. Efficiency and breakdown measurements 43

3.3.1. Results obtained in Russia 43

3.3.2. Results obtained in Austria 47

3.4. Conclusion and outlook 51

A. Logarithmic Units **56**

B. Calculation of the focal distance of a thin lens **58**

C. Energy, power and intensity calculations **60**

Chapter 1.

Propagation principles for optical fibers

In this chapter considerations of light propagation based on a ray model are employed. It is sometimes simplier to regard rays instead of solving wave equations and determining eigenvalues (eigenvalue problems) and then to interpret the results. A very good explanation of wave propagation theory for the conventional step index and graded index fiber can be found in [21] and for the hollow core photonic band gap (PBG) fibers in [3]. This chapter contains a comparison of step index fibers employing the principle of total internal reflection and hollow core PBG fibers employing the principle of multiple reflections. Further, the Gaussian beam is defined and then the methods for characterizing, interpreting and measuring of the beam (quality) emitted from a laser are introduced.

1.1. Total internal reflection

The guiding of light in the conventional step index fiber is based on total internal reflection. That means, the beam is confined in the core having a higher refractive index than the cladding, which additionally protects the core against external damage. To explain the mechanism, first the maximum accepting angle should be found, which allows guiding. It is reasonable to use the Snell's law

$$\sin(\alpha) = n_c \sin(\beta), \tag{1.1}$$

$$n_c \sin(\gamma) = n_{cl} \sin(\delta), \tag{1.2}$$

where n_c and n_{cl} denote the refractive index of the core (c) and of the cladding (cl), respectively. The behavior of a ray is depicted in figure 1.1 with all relevant angles mentioned in (1.1) and (1.2). Angles β and γ are located in a triangle including a 90 degree angle and so $\beta + \gamma = \frac{\pi}{2}$. One can write with $\sin(\beta) = \cos(\gamma)$

$$\sin(\beta) = \sqrt{1 - \sin^2(\gamma)}. \tag{1.3}$$

When $\sin(\delta_{max}) = 1$, for the critical angle of total reflection is defined

$$\sin(\gamma_{max}) = \frac{n_{cl}}{n_c}. \tag{1.4}$$

After insertion in (1.1) and (1.2), it leads to

$$\sin(\alpha_{max}) = \sqrt{n_c^2 - n_{cl}^2} \tag{1.5}$$

$$\alpha_{max} = \arcsin\left(\sqrt{n_c^2 - n_{cl}^2}\right), \tag{1.6}$$

where α_{max} denotes the maximum accepting angle, which can appear when coupling light into the fiber. By this chance, numerical aperture (NA) is introduced:

$$\sin(\alpha_{max}) = \mathrm{NA} = \sqrt{n_c^2 - n_{cl}^2}, \tag{1.7}$$

in the case of the incident beam. Inside the fiber $\sin(\alpha_{max}) = \frac{\mathrm{NA}}{n_c}$ is to be applied.

1.2. Multiple reflections

In the case of a hollow core PBG fiber, the guiding has to be imagined in another way, namely as a sum of many reflections, which can constructive interfere under certain condition. In the case of the conventional step index fiber, for the entering beam there is a maximum off-axis angle when coupling into the fiber. For PBG fiber there is also a maximum angle, called Bragg angle, for which a strong cumulative reflection appears. The Bragg angle is sharply defined according to the mathematical expression (1.8). The principle of propagation is depicted in figure 1.2.

$$\theta_{Bragg} = \arcsin\left(\frac{\lambda}{2\Lambda n}\right), \tag{1.8}$$

where λ denotes the wavelength, Λ the hole interspace (details in figure 1.3), and n the average refractive index.

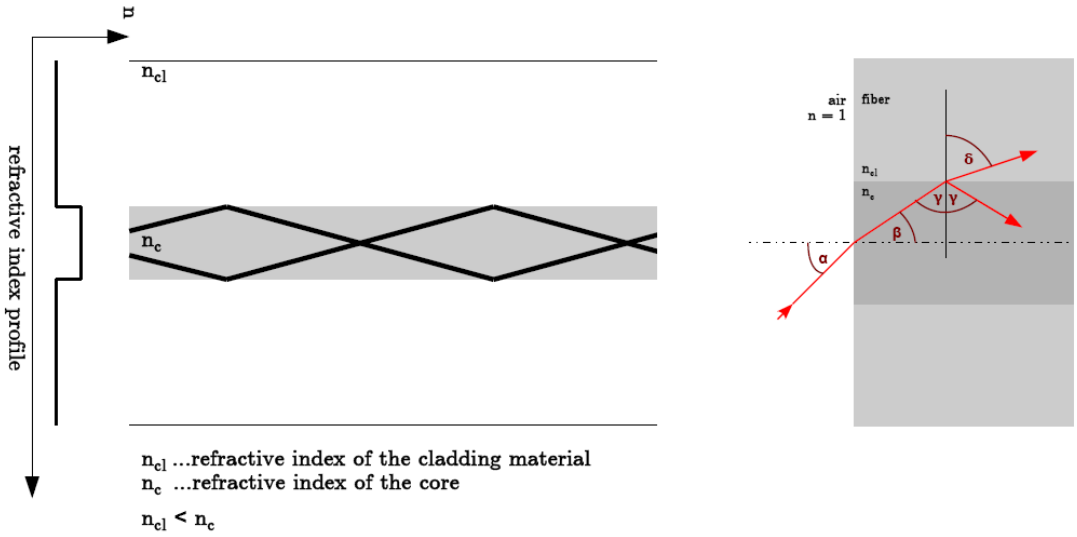

Figure 1.1.: The picture shows a conventional step index fiber. On the left side the refractive index profile together with the guiding principle of a beam is depicted. In the right part of the figure, the principle of total internal reflection is sketched. Total internal reflection appears when $\alpha \leq \alpha_{max}$.

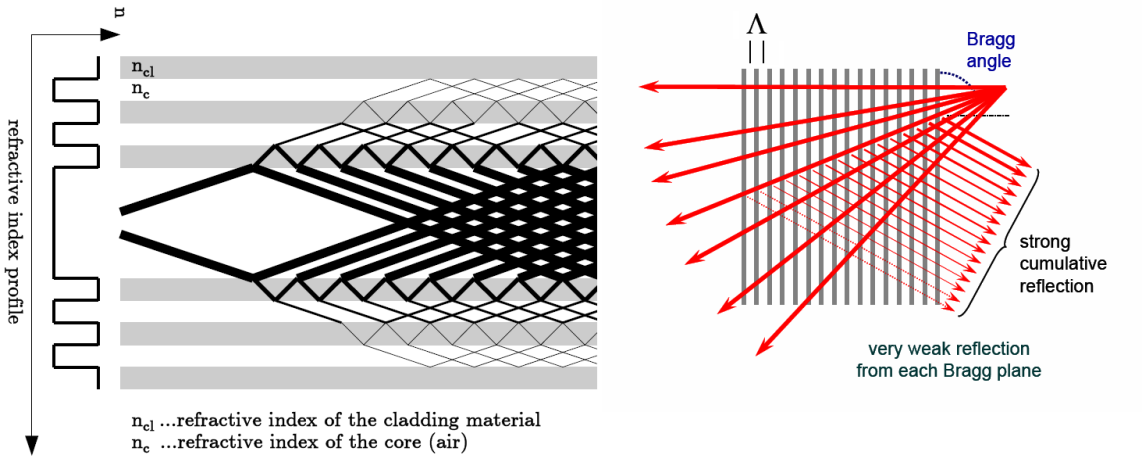

Figure 1.2.: The graphics shows a hollow core PBG fiber. On the left side the refractive index profile with the guiding principle of a beam can be seen. In the right part of the figure, the principle of multiple reflections is sketched as well as the Bragg angle. [26]

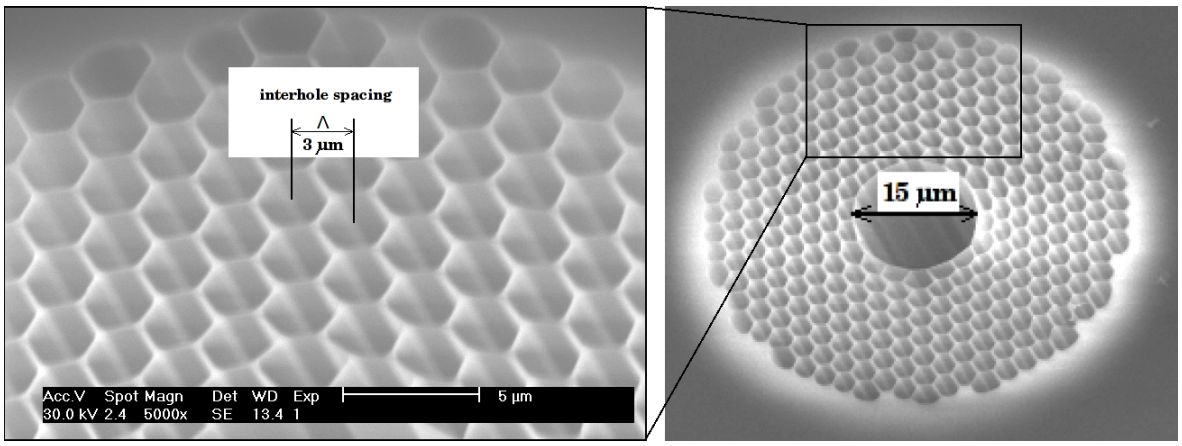

Figure 1.3.: Important characteristic dimensions of the hollow core PBG fiber. The core diameter is 15 μm and the interhole spacing Λ is 3 μm.

1.3. Gaussian beam definition

The diameter of a laser beam changes with the propagation and generally becomes wider on both sides of the waist. To explain the principles and limitations of a laser beam, the consideration of a Gaussian beam is provided. A Gaussian beam possesses a transversal profile as depicted in the following figures 1.4 and 1.5, which can be mathematically expressed in equation (1.9)

$$I(r) = I_0 \cdot e^{-\frac{2r^2}{w^2(z)}}, \tag{1.9}$$

where $r = \sqrt{x^2 + y^2}$ and $w(z)$ denotes the radius of the beam.

The difference between those two figures 1.4 and 1.5 is the defined beam diameter. In the first figure 1.4, the beam diameter is defined as $d_{\frac{1}{e^2}}$, where the intensity drops to its $1/e^2$-value of the initial intensity I_0. 86 % of the complete energy is situated within the interval of -$\frac{d}{2}$ to +$\frac{d}{2}$. In the second figure 1.5, the "full-width half-maximum" (FWHM) beam diameter, termed as d_{FWHM}, is the distance between the two points of the profile, where the intensity falls to its half value of the initial intensity I_0. The amount of energy remaining in the range of -$\frac{d_{\mathrm{FWHM}}}{2}$ to +$\frac{d_{\mathrm{FWHM}}}{2}$ is 61 %. These facts are summarized in the following table.

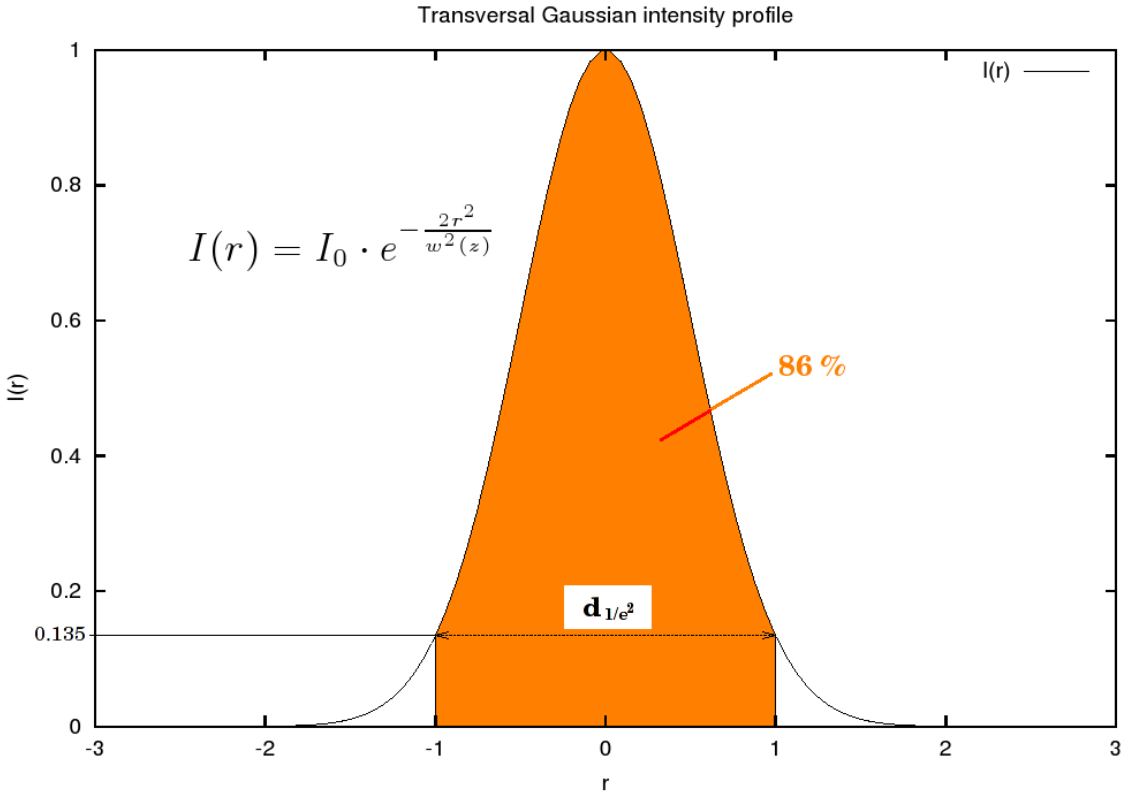

Figure 1.4.: Intensity profile of a Gaussian beam (TEM_{00}) with defined diameter d_{1/e^2}.

	diameter	intensity value	amount of energy
1	d_{1/e^2}	0.13534	85.84 %
2	d_{FWHM}	0.5	61.32 %

The equation (1.9) contains the beam radius $w(z)$, which is dependent on the distance z from the waist w_0, which is expressed with in following mathematical expression (1.10)

$$w(z) = w_0 \sqrt{1 + \left(\frac{\lambda z}{\pi w_0^2}\right)^2}, \tag{1.10}$$

where w_0 denotes the waist ($2w_0 = d_0$) at the point $z = 0$, λ the wavelength and $w(z)$ the current beam radius.

In a representative distance z, termed "Rayleigh range" and indicated with "z_r", the beam radius $w(z)$ increases to the value $w_0\sqrt{2}$. At this point the near field is considered

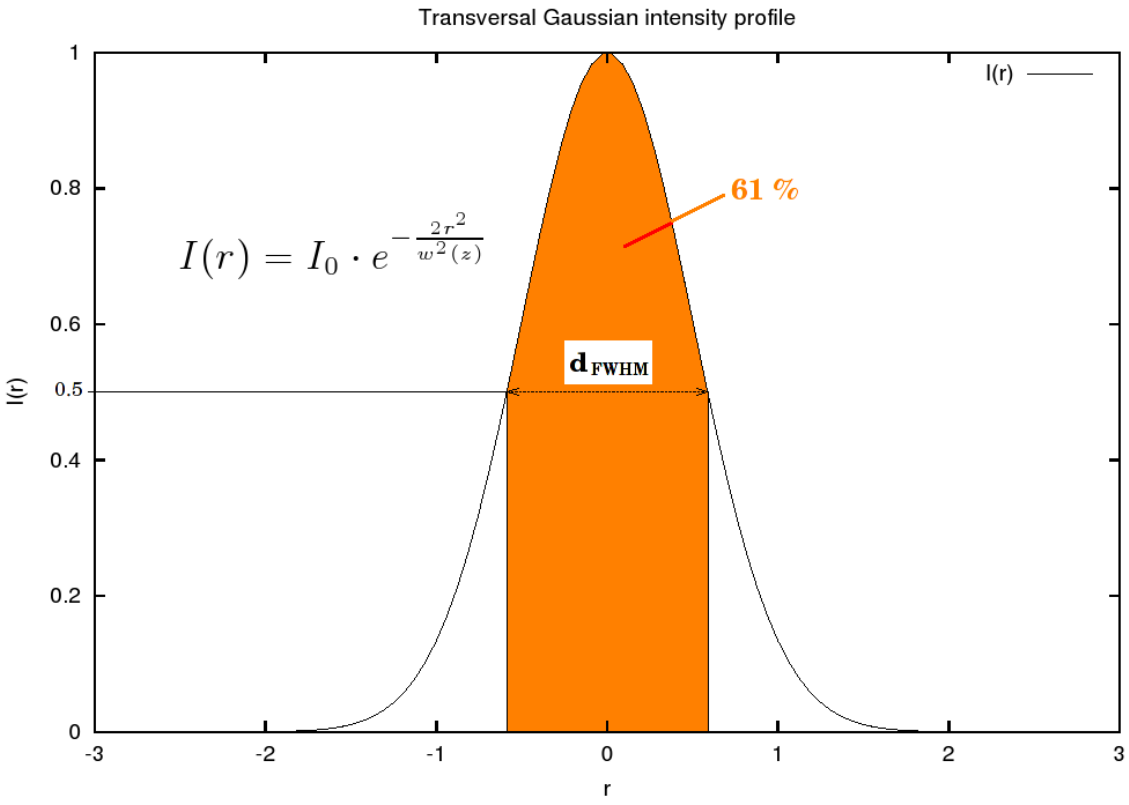

Figure 1.5.: Intensity profile of a Gaussian beam (TEM_{00}) with defined diameter d_{FWHM}.

to change to the far field and at this point the beam possesses its maximum curvature. Then the curvature starts to diminish, so that in infinity the wave becomes again planar as at the position of the waist. In the distance of 10 times the *Rayleigh range* from the waist, the spreading of the beam can be approximated by an angle θ, which defines the divergence of the beam. It is necessary to notice, that θ represents the half aperture angle.

In the next equation (1.11) z_r is defined and in the proximate equation (1.12) the half divergence angle θ is expressed,

$$z_r = \frac{\pi w_0^2}{\lambda} \tag{1.11}$$

$$\theta = \frac{\lambda}{\pi w_0}, \tag{1.12}$$

where θ is not the reciprocal value of z_r, as it appears at the first sight. In the figure 1.6 beneath, the complete behavior of a Gaussian beam is depicted.

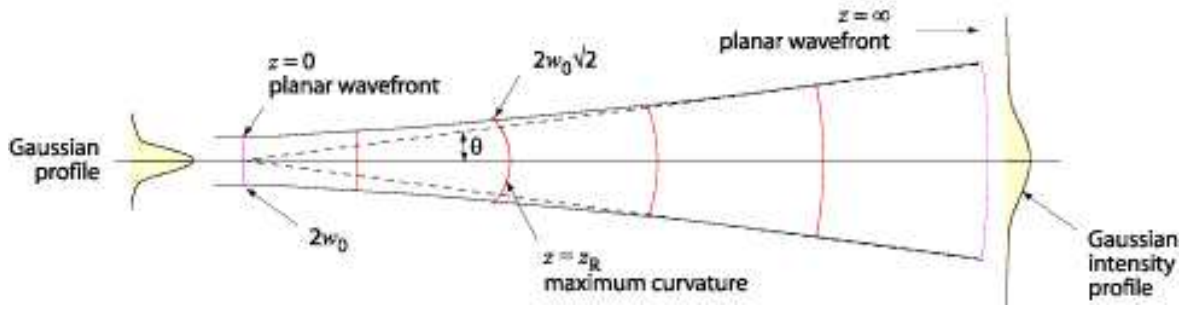

Figure 1.6.: The behavior of an ideal Gaussian beam, which is always symmetric around the waist w_0.

1.4. Quality of the laser beam and M^2

There have been many efforts to characterize the beam quality of a laser. The best alternative would be a universal simple method, easy to measure, applicable on every real laser beam, which is useful in designing and analyzing. One such characterization is expressed by a single number, the so called "M-square" (M^2), which applies to beams with spherical diameter, e.g. non-astigmatic. It has to be mentioned, that the near-field size and the far-field beam spread has to be regarded, in order to get a good estimation of the beam quality. For simple imagination, a high quality laser beam should be marginally divergent and well focusable. The parameter M^2 provides a comparison between the ideal Gaussian beam and the real beam. The ideal Gaussian beam possesses $M^2 = 1$ predefinition and a real laser beam always has M^2 greater than 1. Mathematically, the diffraction limit looks like

$$\theta w_0 = \frac{\lambda}{\pi}, \tag{1.13}$$

where θw_0 is invariant and depends only on λ. In comparison with a real beam, which possess also an invariant relation ΘW_0, M^2 can be introduced as

$$\frac{\Theta W_0}{\theta w_0} := M^2 > 1, \tag{1.14}$$

which implies, that M^2 is a value denoting how many times the diffraction limit fits into the real beam.

Measurements of M^2 show more information about the beam quality than only a visual fit estimation. Having determined M^2, focusability of the beam can be predicted more easily and more precisely. This becomes important, when it is necessary to choose a series of focusing lenses, where accuracy of some μm is needed, whether professional software for focal spot size estimation is used or not. In the figure 1.7 one can see the computational calculation of the focal spot radius for an aspherical lens of focal length of 7.5 mm. The focal distance depicted on the left side becomes 9.736 mm, because the laser beam does not fill the total lens aperture and this means also that the NA (numerical aperture) changes from its original value of 0.3 to 0.1643. In the table, there are many useful values (all units are in mm), but only the value indicating the diffraction limit is of interest. With the information about M^2 (for the laser "Litron" $M^2 = 1.54$) one can estimate that the focal spot diameter is $\simeq$12 μm by using the diffraction limit value computed by a software as the waist w_0 (3.928 μm, see figure 1.7). Multiplication with M^2 takes a real beam into account and so the radius of the spot becomes 6 μm and thus the spot diameter 12 μm. In the following, some measurement methods are listed.

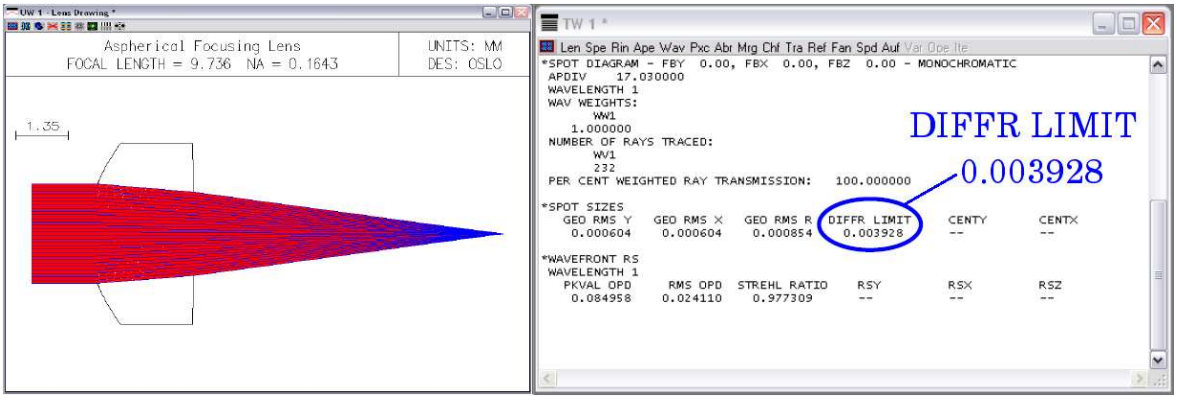

Figure 1.7.: Computational calculation of the focal spot.

1.4.1. "Second moment" method for determining of M^2

This method for determination of diameters of real laser beams was standardized by ISO (International Standards Organization) and is based on the propagation theory by A. E. Siegman. [29] First there have to be defined the mean location $(\overline{x}, \overline{y})$ of normalized intensity distribution $I(x, y)$ and the mean angular orientation $(\overline{\theta}_x, \overline{\theta}_y)$,

$$\overline{x} = \int\int x I(x,y)\, dx\, dy \tag{1.15}$$

$$\overline{\theta}_x = \int\int \theta_x I(\theta_x, \theta_y)\, d\theta_x\, d\theta_y. \tag{1.16}$$

For the y-plane, the equations (1.15) and (1.16) are analogous. The propagation axis for the beam is a straight line in the space composed of location of the center and the angular orientation. Henceforth the beam width and the divergence angle can be defined and measured as the standard deviations σ. For the x-plane the expressions are

$$\sigma_x^2 = \int\int (x - \overline{x})^2 I(x,y)\, dx\, dy \tag{1.17}$$

$$\sigma_{\theta x}^2 = \int\int (\theta_x - \overline{\theta}_x)^2 I(\theta_x, \theta y)\, d\theta_x\, d\theta_y. \tag{1.18}$$

So the beam diameter d_x (analogous for d_y) and full divergence angle Θ_x (analogous for Θ_y) become

$$D_x = 4\sigma_x \tag{1.19}$$

and

$$\Theta_x = 4\sigma_{\theta x}. \tag{1.20}$$

According to the theory, there is a variation of the beam diameter along the propagation axis z corresponding to

$$D^2 = D_0^2 + \Theta^2 (z - z_0)^2, \tag{1.21}$$

where D_0 denotes the tightest diameter of the beam called beam waist, when z equals z_0, which is the position of the waist on the z - axis. It has to be noticed, that the equation above can be applied generally for all field distributions and is not limited merely to a specific field distribution. That means that every light beam can be approximated by a hyperbola. Further, this fact was used in experiments for determination of M^2 of two flash lamp pumped, Q-switched Nd:YAG lasers, which are in use for the purpose of

igniting gas mixtures in internal combustion engines. The results of these experiments can be seen in chapter 3.2.

For an ideal Gaussian beam M^2 equals 1, which denotes the bottom limit for real beams. A real beam always possesses $M^2 > 1$. In similar consideration real beams

a) diverge faster by the factor M^2 for a given radius or

b) have the same divergence angle (θ) but larger waist by M^2 or

c) diverge faster by M ($= \sqrt{M^2}$) and simultaneously have larger waist by M,

which is depicted in the figure 1.8 on the page 11. The product of divergence angle and waist, in case of phase fronts of perfectly spherical forms $M^2 = 1$, is accurately described by

$$D_0\Theta = M^2 \cdot \frac{4\lambda}{\pi}, \tag{1.22}$$

and the above mentioned items a), b) and c) can be written as mathematical interpretations

a)
$$D_0\Theta = d_0(M^2\theta) \tag{1.23}$$

b)
$$D_0\Theta = (M^2 d_0)\theta \tag{1.24}$$

c)
$$D_0\Theta = (Md_0)(M\theta). \tag{1.25}$$

The fact should not be forgotten, that there are additional potential sources of error, like

- non-trivial calculation of the second-moment diameter

- background noise and quantization noise due to limited dynamic range of the ADC (Analog Digital Converter)
- non predictable abnormal behavior of an intensity profile

which can be surmounted in well designed measurement systems. Software designers try to develop software which can manage some adjustments automatically.

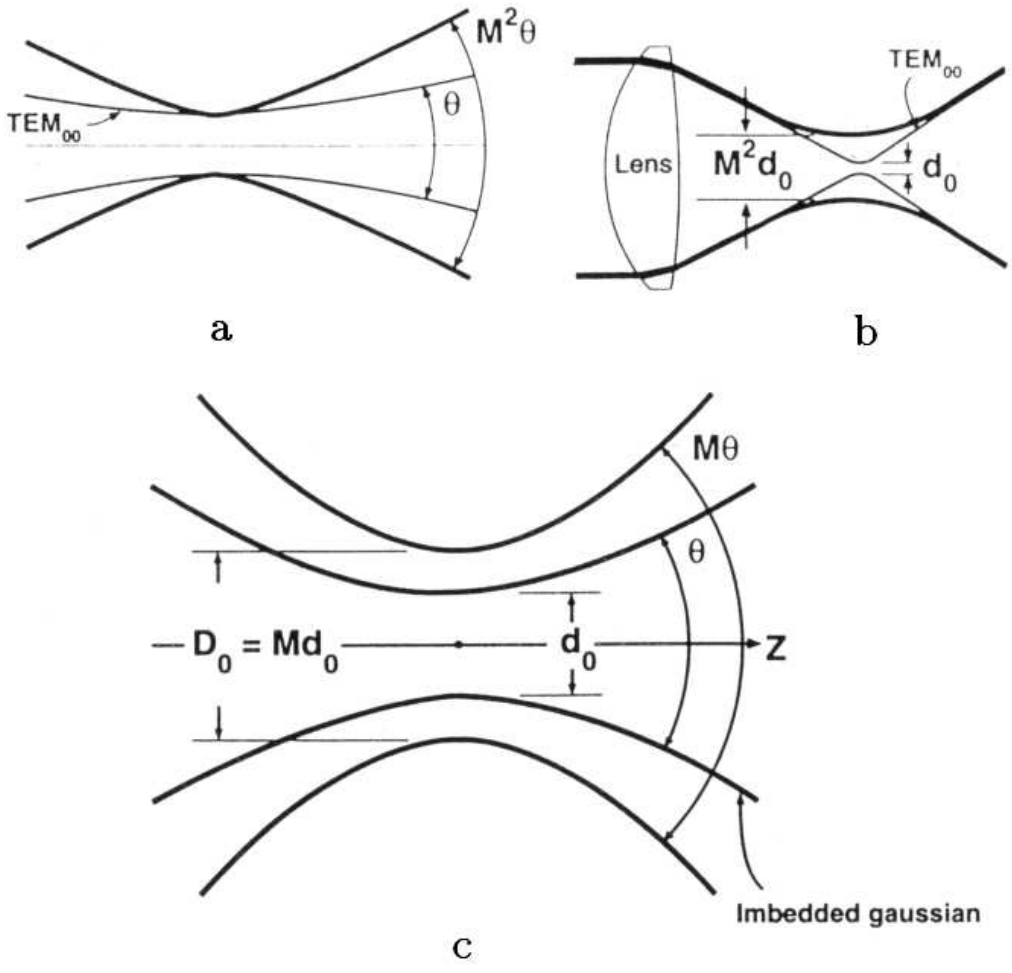

Figure 1.8.: Real beam versus ideal beam.

1.4.2. Scanning slit method for determination of M^2

With the help of a narrow slit installed between the beam and a fixed large-area photo detector an intensity profile can be recorded directly without differentiation or filtering

due to the fact that the slit functions as a natural attenuator, which allows only a fraction of the laser energy to pass through onto the detector. The profile of the beam is taken from the photon current versus distance and the clip level is defined as the distance between the 13,5 % values, which corresponds to 100 % of the irradiation. The scanning slit method is aligned easily and gives a relatively good spatial resolution of the real beam structure. As one can imagine, in the case of a Gaussian beam this method may be very good, but for real beams the diameter measured by this method is smaller than the real one. Figure 1.9 (page 13) displays the data received by this method.

1.4.3. Pinhole method for determinination of M^2

Like in the scanning slit method a pinhole is placed between the beam and the photo detector instead of a slit. The profile can be reconstructed from the relation of the current versus distance. Although this method may provide one of the best spatial resolutions, the alignment difficulty rises with same grade as the resolution. The pinhole has to cross the peak of the laser beam, which is a comparably heavy task in focused beams. Nevertheless, it is preferred to use this method instead of the scanning slit method. After taking a two-dimensional array of data one of three methods for analysis can be applied: slit, knife edge or variable aperture method. Obtained data by such methods is depicted in figure 1.9 on page 13.

1.4.4. Knife edge method for determinination of M^2

This method demands differentiation and filtering to obtain the profile. Between the laser beam and and a photo detector a knife edge is installed. The knife-edge scan (photon current versus distance) has to be differentiated first to observe a profile. Because of the high amount of energy, a filter has to be placed in front of the detector, in order to prevent saturation or even destruction. The incorrect usage of filters can cause a thermal lens, which increases the actual measured beam. This method is used for submicron spot size measurements and is regarded as the most practical one. The result of a measurement by knife edge method is shown in figure 1.9.

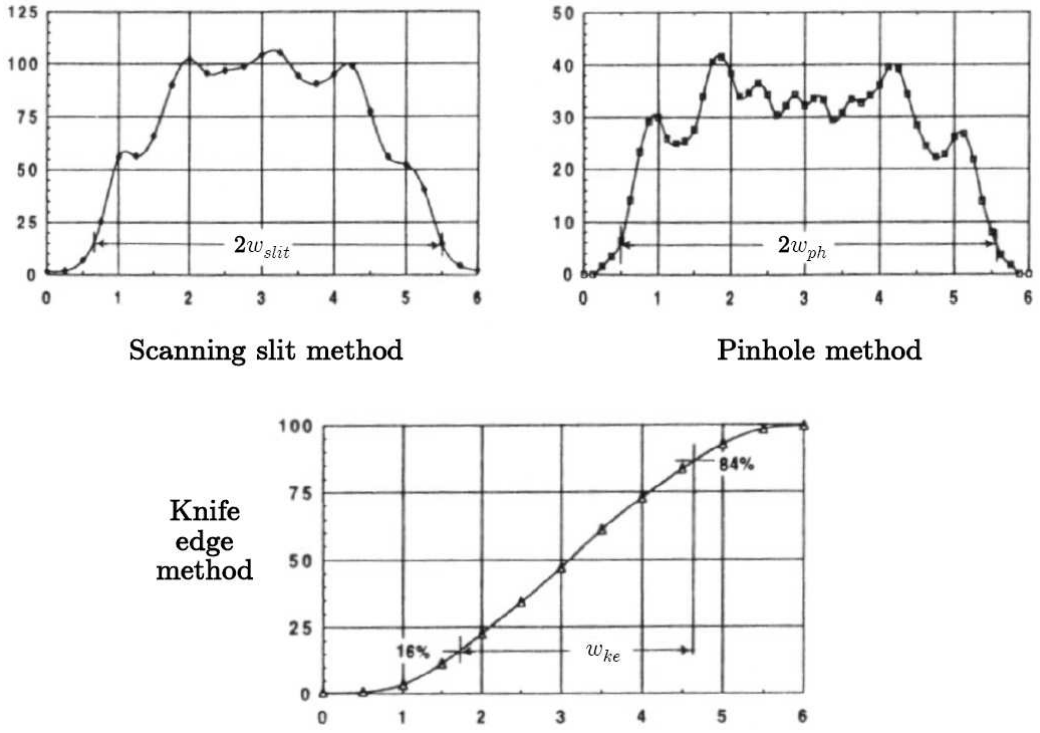

Figure 1.9.: Examples of received data by different methods.

1.4.5. CCD - Charge Coupled Device used for determination of M^2

This method is based upon using a CCD camera, consisting of CCD arrays. The range of wavelengths that can be captured is huge and goes from around 200 nm in UV to over 1100 nm in near IR (Infra Red). The resolution of such beam profilers depends on the dimension of the array and the size of the pixels. The smaller the pixels the tighter beams can be examined, and the greater the dimension of the array the wider beams can be analyzed. In most cases the beam profilers are able to measure spot size, position and relative energy, calculated with an included supportive software. It is not difficult to imagine that these devices are highly sensitive, so that high grade and quality filtering has to be provided, and in majority of cases, the manufacturer offers combinations of profilers and sets of tunable filters. This method tends to be most cost effective. Figures can be seen in chapter 3.2. termed "M^2 of the laser", where measurements with beam profilers were performed.

Chapter 2.

Experiments

In order to get precise results some important precautions have to be met. First of all, preparations for experiments determine the results afterwards. After careful preparations the measurements can start. The optical fiber used in the experiments is a photonic band gap fiber, also called photonic crystal fiber, because of the periodic structure around the hollow core, which forms a two-dimensional photonic crystal. As mentioned before, the hollow core provides the guiding of waves and has to be without damage or distortion by glass particles produced by cleaving. Tight focusing has to be done, so that nearly the complete energy can fit into the hollow core. Therefore the surface of the fiber has to be as even and smooth as possible. Correct methods of analyzation have to be chosen to get expressive results, such as using CCD-camera for visualizing the coupling process. On top of all, pictures from the beam profiler, using a light microscope and an environmental scanning electron microscope round off the complete effort.

Since the experiments were done at two different places, namely, as a part of an exchange project at the Lomonosov Moscow State University (Chair of General Physics and Wave Processes) in Russia and at the Vienna University of Technology (Photonics Institute) in Austria, the chapter dedicated to results will be divided into two fractions. Where the split-up is not relevant, a referring notice is given.

2.1. Experimental setup

At the beginning of this work the experimental setup had to be configured and then constructed. For the experiments the following devices and parts were needed

- ⇒ PBG Fiber
- ⇒ Laser
- ⇒ Visible laser pointer
- ⇒ Laser protection glasses
- ⇒ 4 mirrors (totally reflective for $\lambda = 1064$ nm)
- ⇒ 2 sapphire windows (for the vacuum chamber)
- ⇒ Three-dimensional micro-positioning stage with fiberholder
- ⇒ Series of focusing and collimating lenses
- ⇒ Vacuum chamber
- ⇒ Various detectors for IR laser emission, energy and beamprofile.

PBG Fiber The original name of the PBG fiber is HC19-1060-01. HC denotes "Hollow core", 19 is the number of cells omitted, which represent the hollow core, and the the fiber is designed for the wavelength of "1060" nm. In the following figure 2.1 one can see the surface of such fiber after classical cleaving.

Laser The ambition to transmit high power laser pulses through a fiber originates from the project termed "Laser Ignition". For laser ignition, high power flashlamp-pumped Q-switched Nd:YAG (neodymium-doped yttrium aluminium garnet, Nd:$Y_3Al_5O_{12}$) lasers with typically 6 ns pulse duration are in use and their characteristic emission wavelength lies at 1064 nm in near IR. For this reason the PBG fiber is also designed for the wavelength of 1064 nm. For various experiments 2 different Nd:YAG lasers were used. One, located in Russia, was actively Q-switched and designed to emit 1064 nm radiation

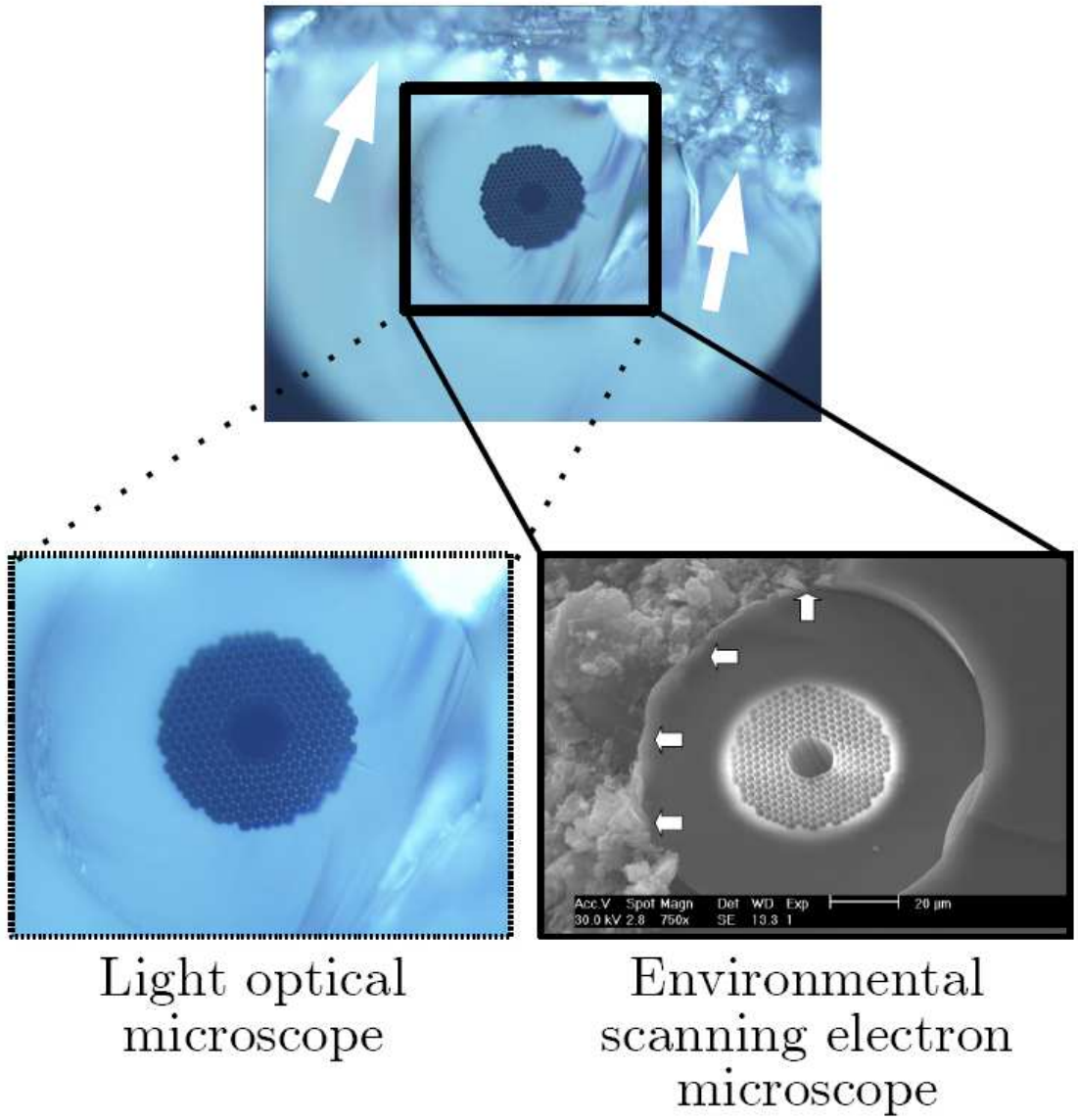

Figure 2.1.: The upper picture shows the 50 times magnified surface of the fiber taken by a light optical microscope. The enlargement on the lower left hand is also captured with a light optical microscope using 100x magnification, depicting the cladding with the periodical structure and the hollow core. The picture on the lower right hand was obtained by the environmental scanning electron microscope. The arrows point out the cleaving line.

with a pulse duration of 10 ns and a maximum pulse energy of 100 mJ at a repetition rate of 2 Hz and the other one, located in Austria, used an active Q-switch as well and emitted 1064 nm pulses with a 6 ns duration and a maximum pulse energy of 30 mJ with a variable repetition rate up to 50 Hz.

Laser pointer Due to the fact that infrared radiation is not visible for a human eye, but it is focused to the retina in the same way as visible light, an aligning laser pointer was installed. It emitted coherent light at 532 nm, thus green light, which the eye is very sensitive for. This laser pointer was adjusted to the main laser in a way to irradiate the same point on the focusing lens, which is shown more in detail in the adjacent section "Alignment". The pointer primarily served for alignments done without the main laser and hence without protection glasses and for fast coupling trials and collimating lens calibrations.

Laser protection glasses As mentioned before, the infrared radiation of the main laser is dangerous for the human eye, because the light is invisible and focused to the retina and can on that account cause irreversible damage.

Mirrors For the guidance of the laser emission mirrors have been used creating total reflection for the beam, but were only partially reflective for the green emission coming off the laser pointer. One mirror was placed where both beams came together. The second one deflected the beam into the vacuum chamber through a sapphire window. The remaining 2 mirrors were positioned inside of the chamber as depicted in figure 2.2.

Sapphire windows Only windows allowed the beam to enter the vacuum chamber. Sapphire windows were selected because of their temperature resistance capability. On the other hand they produced energy losses that climbed up to 15 %. In Russia instead of sapphire windows, glass windows were used, which caused less losses in the range of 8 %, but the microscope objectives used for focusing and collimating introduced losses of more than 18 %.

Three-dimensional micro-positioning stage For the positioning of the fiber to the focused beam a 3D stage was used. In this way the fiber fixed on a holder could be moved and the focusing lens was attached to a non movable part of the stage. Because of the fixed position of the lens, the focal spot remained at the same point, so that beam alignment had to be done only once. In Russia however, another method was applied, where three-dimensional positioning lens-holders were used, for fixating the fiber. Hence once breakdown happened, new alignment had to be performed. Detailed explanation takes place in separate sections, namely "2.2 Alignment" and "2.5 Coupling".

Lenses The selection of focusing lenses depends on the size of the focal spot and the numerical aperture. Both focusing and collimating lenses were single aspherical lenses, not only because their properties are excellent but also because of the lack of space. For focusing, lenses with 4.5 mm, 7.5 mm and 11 mm focal length were used and for collimating a 11 mm lens proved to be the best choice in interaction with the CCD-camera and the beam profiler. In Russia, microscope objectives with 10x and 20x magnifications substituted the aspherical lenses.

Vacuum chamber In the figure 2.2 the vacuum chamber with the inner construction is depicted. The ability of evacuating the hollow core of the fiber gave rise to the hope, that evacuated hollow core PBG fiber would be able to transmit high power pulses and thus the evacuation chamber was installed to examine that fact. The chamber construction consists, additionally to the ground plate, of an inner plate which largely compensated the bending of the ground plate. Although the ground plate was composed out of aluminum with a thickness of 2 cm, a bending of approximately 20 μm was observed when starting the evacuation due to the established pressure difference. This deviation could not be corrected by the recalibration of the mirror, which deflected the beam into the chamber. The inner plate helped to solve that problem as far as the adjustment of the mirror could correct the deposition of the focal spot out of the hollow core and thus the pressure difference became irrelevant.

Detectors Visualization of the coupling process was performed with a CCD-camera. This method guaranteed a fast coupling with high precision. For verification of the visualised picture the beam profiler was applied. The beam profiler was also used to

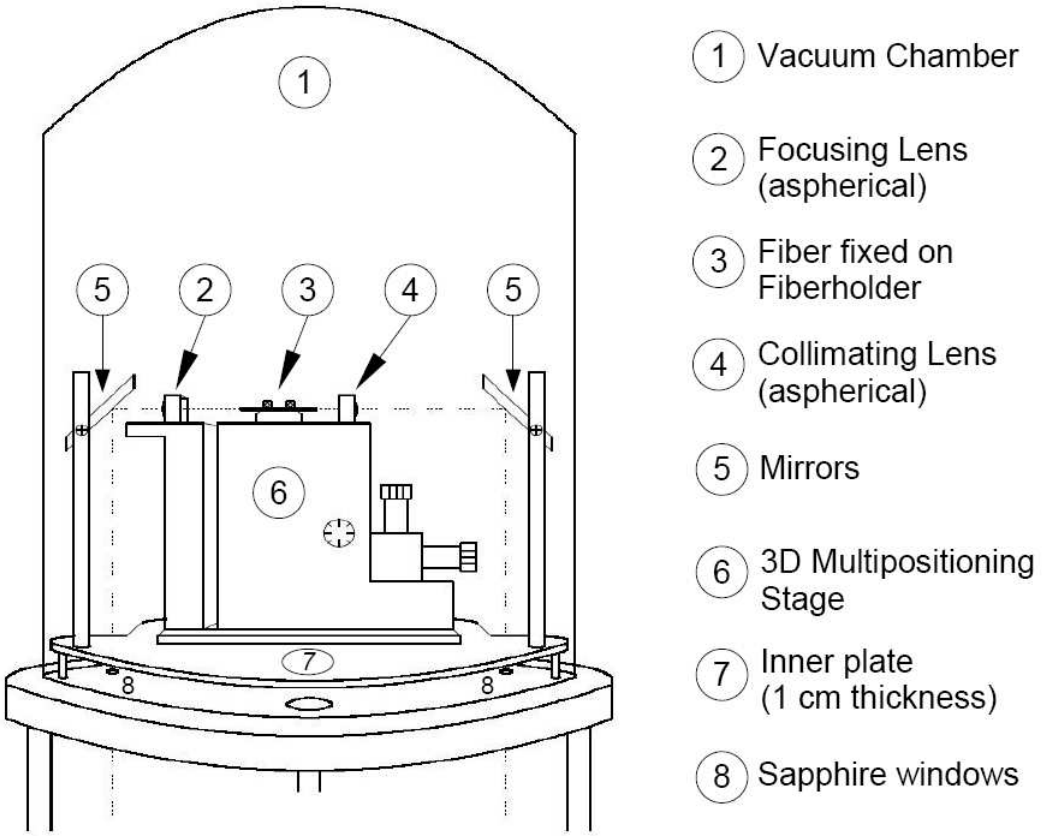

Figure 2.2.: Experimental setup.

gather all the information and properties of the laser beam for the M^2-calculation. The energy detector completed the measurement equipment. To visualize the infrared beam a special detection plate was used, which illuminated when light with a wavelength of 1064 nm impinged on it.

2.2. Alignment

To pay attention to one of the most important aspects such as alignment, a separate section is created. It is divided into two parts, dedicated to two different methods of beam guidance into the fiber. However in both methods the precise delivery of the beam and alignment plays an important role. If a laser beam misses the center of the focusing lens or the microscope objective, the direction of the focused beam and hence the position of the focal spot changes, which can cause intensity peaks on some areas

of the hollow core wall and by this the breakdown of the fiber. The figure 2.3 on the page 20 demonstrates the fact of a misalignment and changed spot positions. With the help of a software OSLO, 0, 5 and 10 degrees deviation off the axis were calculated. The green colored beam displays the proper path of the beam and the accurate position of the spot. The breakdown of the fiber due to a misalignment is shown in the figure 2.4 on page 21.

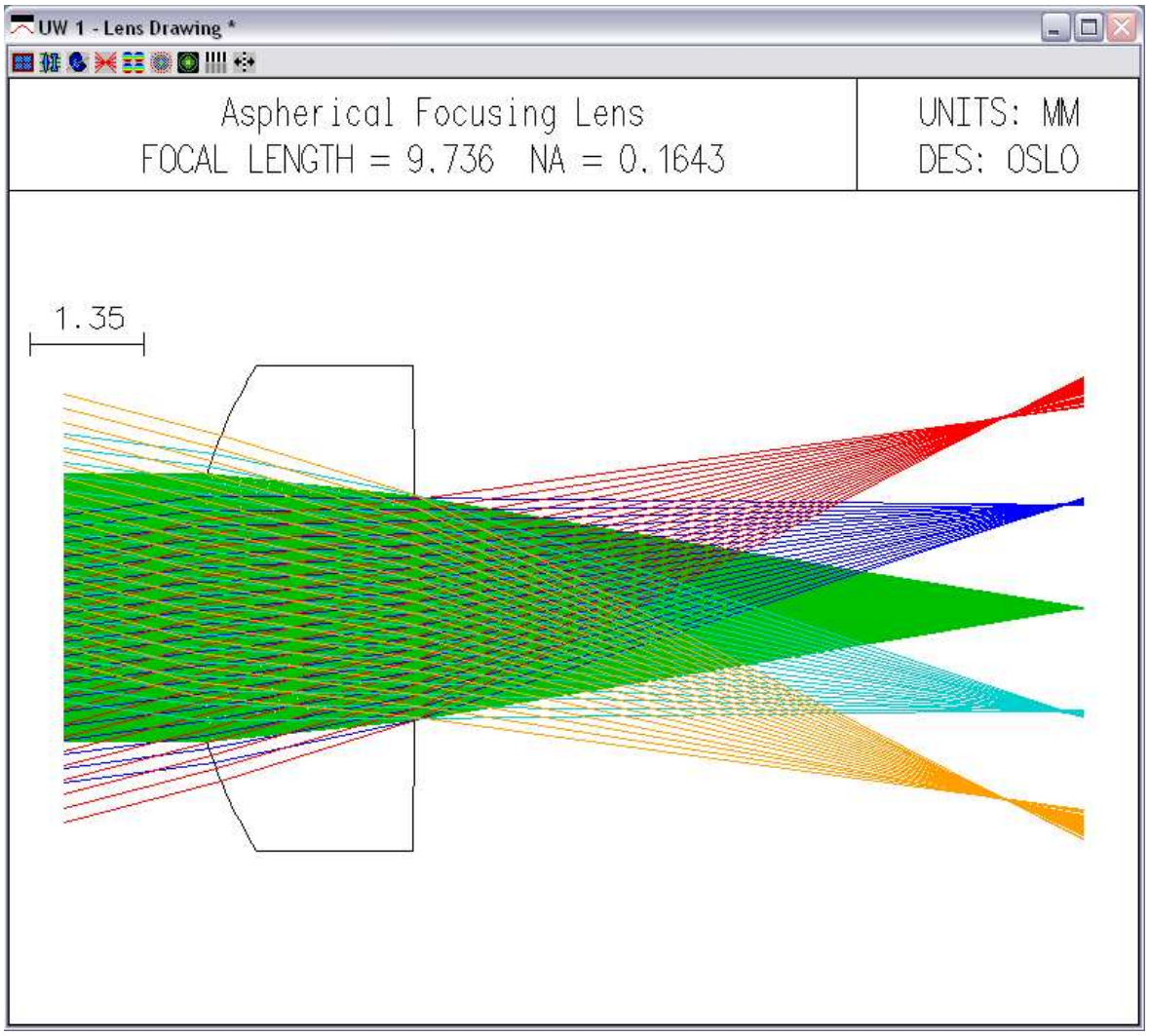

Figure 2.3.: Changed position of the focal spot by misalignment, calculated by the software OSLO.

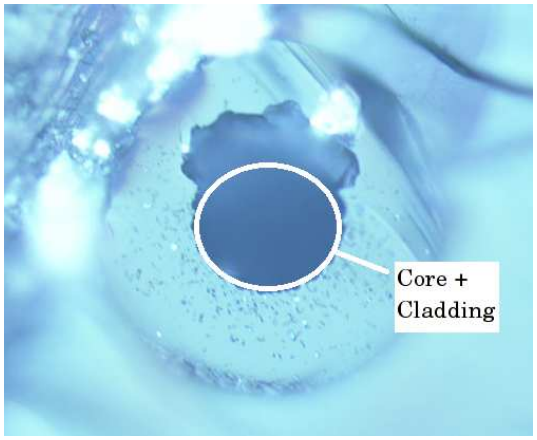

Figure 2.4.: Breakdown of the fiber due to a misalignment.

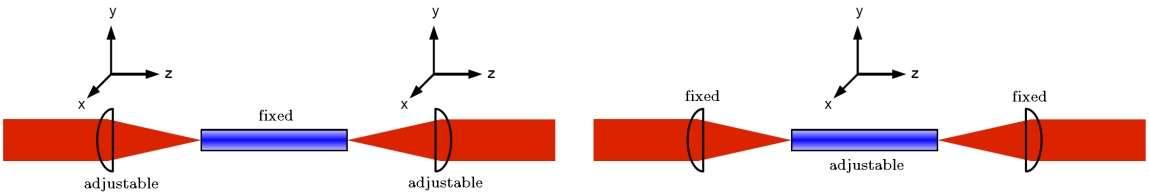

Adjustable microscope objectives and fixed fiber

Fixed aspherical lenses and adjustable fiber

Figure 2.5.: Different coupling methods.

2.2.1. Adjustable microscope objectives and fixed fiber

To provide correct alignment the first step was to let the laser beam pass through the centers of both windows of the vacuum chamber. Then a point of the size of the beam was drawn on a fixed plate. Thereafter the focusing microscope objective was installed. By moving it forward and backward from its selected position, the center of the spot had to remain in the same position, which was previously indicated by the sketched central point on the fixed plate. Then fiber fixed on a holder could be placed into the chamber. This procedure was concluded by the positioning of the collimating microscope objective, which could be aligned by the same procedure as the focusing objective. After each experiment the whole addjusting procedure had to be repeated. This fact was observed in some experiments where no fundamental mode was transmitted through the fiber without repeating the alignment at least of the focusing objective. The explanation is simple. During the coupling process the position of focusing objective changed and after the removal of the broken fiber, the objective itself was decalibrated in a way that the

focal spot did not match with the sketched center point of the unfocused laser. This method can be regarded more time-consuming than the following one.

2.2.2. Fixed lenses and adjustable fiber

This method was used where the laser beam had to be deflected into the vacuum chamber, which is depicted in figure 2.2 on page 19. This method is different to the one used in Russia. Once it was verified that the laser beam hit the center of the focusing lens, no re-alignment was needed any more in case of experiments done under normal air pressure. In case of performed evacuation and calibration by moving the position of the outside positioned mirror, the afore mentioned alignment had to be repeated again. Such alignment took only several minutes time because the original postion of the mirror had to be reached, which indeed was accomplished faster than in the method described in section 2.2.1 before. In this case the aspherical lens was fixed on a non-movable part of the three-dimensional micro-positioning stage. The fiber was fixed on a fiber holder designed especially for this stage, which was located on the movable part of the stage. The collimating lens was fixed behind the fiber on the movable part of the stage as well, which entailed in a simple one-dimensional adjustment of the lens along the propagation direction of the beam.

2.3. Selection of focusing lenses

Tight focusing had to be performed, so that the laser beam fit into the hollow core of the fiber. A simple approximation calculation using the following equation

$$f = \frac{d_{spot} d_{beam} \pi}{2\lambda} \tag{2.1}$$

resulted in a focal length of 8.26735 cm, supposing a 5 mm diameter of the laser beam and a 10 μm diameter of the spot[1]. This could only be in the case of an ideal Gaussian beam and an ideal spherical surface of the lens. Both properties are not ideal in practice.

[1] The complete calculation is performed in appendix B

In case of an ideal surface of the lens but with a real beam, manifested by M^2 of 1.54, the value dropped down to 5.82208 cm, but it still remained non-realistically high. The material property of the lens defines if the laser beam can be focused this tight. Most lenses, in the case of the aspherical lenses as well, are manufactured of a material which is designed to a wavelength of 810 nm, in the case of 7.5 mm lens, and 670 nm in the case of 11 mm lens, and causes losses and reflections in case of other wavelengths. Further, high peak power pulses can generate non-linear effects, such as thermal lensing, which also changes the focusability of the beam. A computational calculation shows the dependence of the spot diameter and numerical aperture (NA) on the diameter of the laser beam in the figure 2.6. There was already a previous attempt to use a single aspherical lens with the focal length of 7.5 mm. Indeed such a lens would focus the beam to a small-sized spot of less than 10 μm diameter when using a laser with a beam diameter of 5.8 mm. In the beginning of the experiments such a laser was available, namely Quantel Brilliant. The specified numerical aperture of the 7.5 mm focusing lens was 0.3, which was a value greater than the NA of the fiber, estimated to be 0.1586. As a consequence, losses occured and not all of the energy could propagate in the hollow core. Because of this, another lens was chosen to be the focusing lens. This lens had a focal length of 11 mm and NA of 0.3, but it had a greater aperture of 6.6 mm, which effectively lowered the NA using a laser with the same diameter. For reasons of "Quantel" being used in other experiments, "Litron" became the main experimental laser. After the replacement of the laser, the laser beam diameter changed too. There was the need to find out if the smaller beam of 3.2 mm diameter would be able to be focused into the core without touching the walls. It was found out, that the lens with the focal length of 7.5 mm fulfilled the condition of having a smaller focal spot than the diameter of the core, but caused a greater NA, as it is depicted in the figure 2.6. Therefore, the lens with the focal length of 11 mm produced a focal spot diameter of 17.06 μm, but the NA had a lower value than 0.1586 of the fiber. This was experimentally determined by the ratio of output energy to input energy resulting in a value of 80 %. For simpler explanation, one has to imagine a funnel. Filling it with an amount of water is the same as using a lens with a laser beam with a diameter causing a greater NA. If the water in the funnel is overflowing, it means that the amount of water is too high. If the effective NA of the focusing lens is higher than the NA of the fiber, it means that the complete energy cannot be coupled into the core of the fiber. The following table summarizes the global values from the selected aspherical lenses used for focusing.

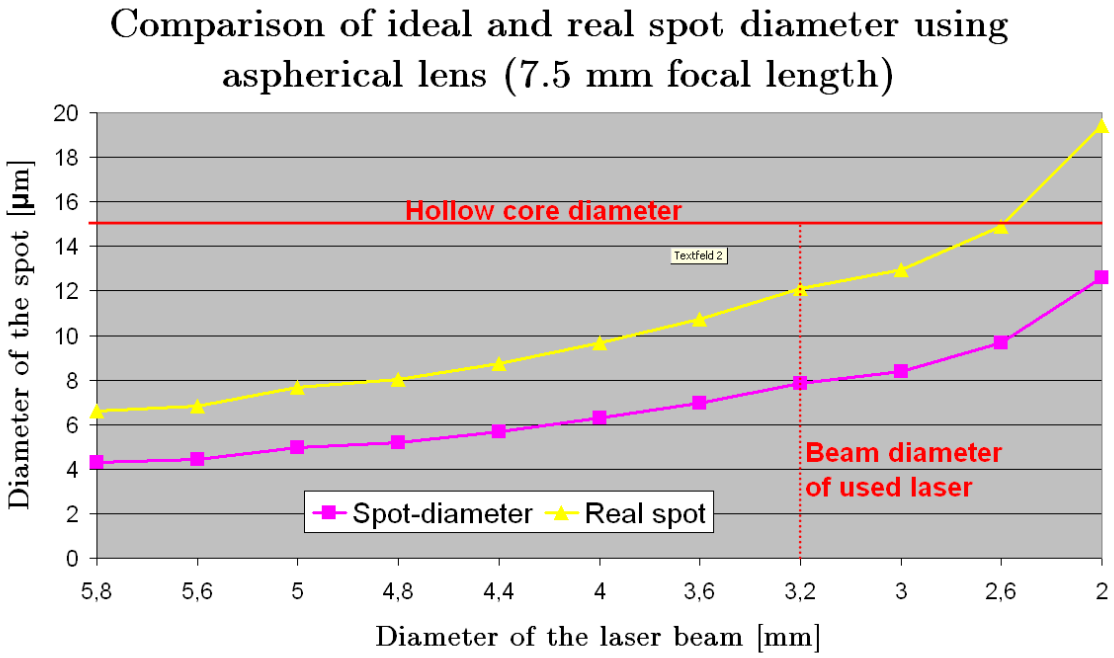

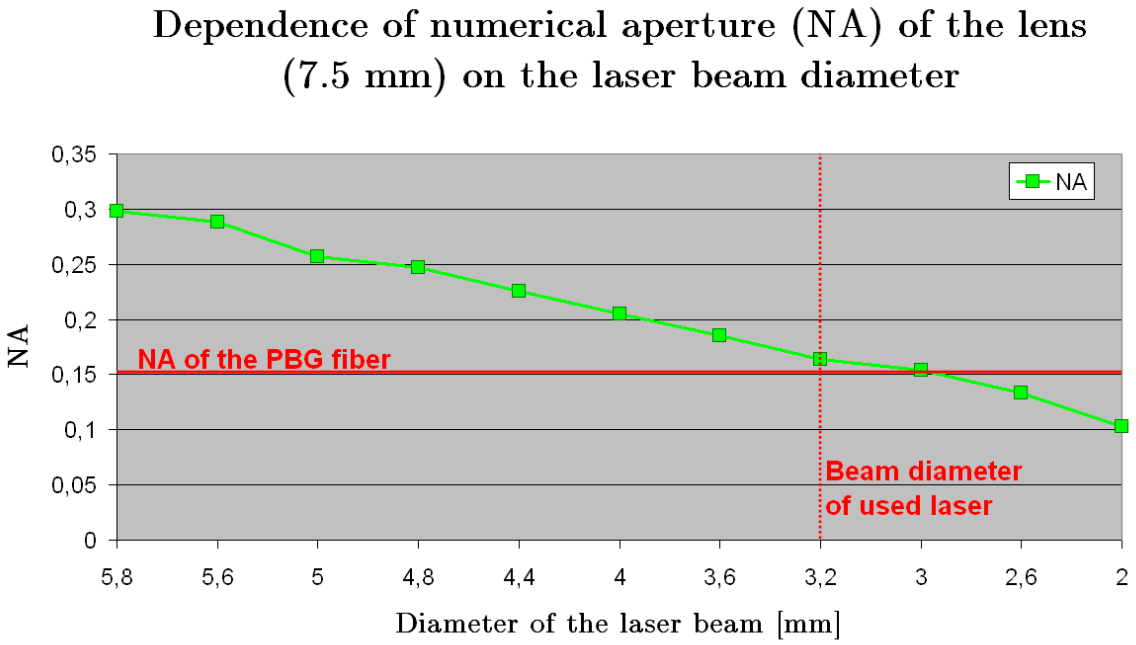

Figure 2.6.: Effects on the spot diameter and NA caused by the variation of the laser beam diameter. Spot diameter should be lower than the diameter of the hollow core, and the numerical aperture (NA) should also be lower than the NA of the fiber as sketched by the red lines.

focal length	designed for λ	aperture	NA	spot diameter	effective NA
7.5 mm	810 nm	6 mm	0.3	12 μm	0.1643
11 mm	670 nm	6.6 mm	0.3	17 μm	0.1151

2.4. Cleaving

One of the most important aspects remains: the cleaving of the hollow core PBG fiber. Especially because of the hollow core, conventional cleaving fails. Using conventional cleaving some broken parts and particles from the cladding would be introduced into the hollow core and cause a major reduction of the transmission. Beside that significant fact, the cladding forming the two-dimensional photonic crystal by conventional, which is also definitively responsible for the appropriate guiding by creating a multilayered mirror for the electromagnetic wave, would be destroyed by conventional cleaving.

The fiber for the experiment was split in the same classical way as glass is split. First the protective coating was scratched by a so called "Sapphire Proscribe". It is not necessary to remove the coating to achieve better results. The removal can additionally cause damage to the fiber and takes several minutes of very careful and thus exhausting work. The "pen" consists of a sapphire blade, which possesses a 60 degree wedge shape allowing the user to cut from both sides [12]. In the figure 2.7 there is the picture of such a cleaving device and below that is the sketch of wounding the coating in a proper way to obtain the best splitting results.

Figure 2.7.: "Sapphire Proscribe" used for wounding the coating and cladding to cleave the PBG fiber.

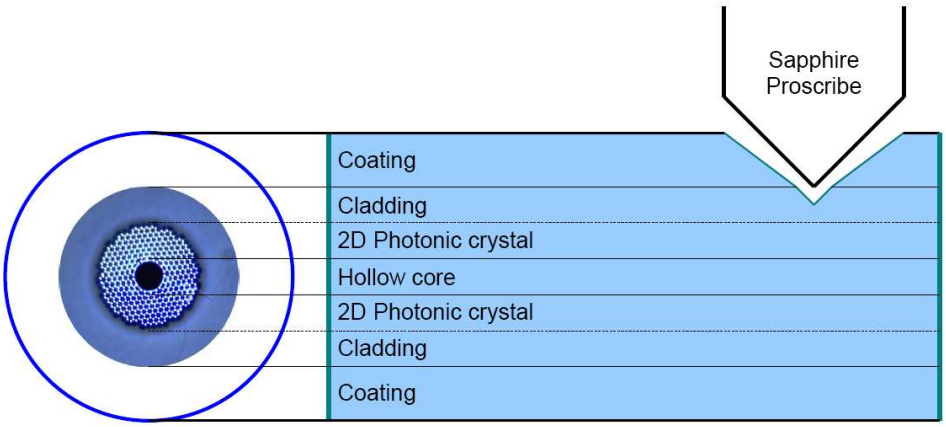

Figure 2.8.: Sketch of the cleaving procedure.

2.4.1. Procedure of cleaving

First the fiber has to be placed on a planar surface. A table surface is sufficient. For a better view on the fiber a white sheet of paper can be used. After placing the fiber on the table, one hand (finger) fixes the fiber, so that it cannot move. With the "sapphire proscribe" the coating is wounded in following way: Perpendiculary and after contact to the fiber, the "sapphire proscribe" is moved forward and backward with applied light pressure toward the fiber as depicted in figure 2.9. It has to be noticed, that a length of the piece, which is one third longer than the fiber holder, has to be chosen before contacting the fiber. This is necessary for saving purposes. 2.5 cm of the PBG fiber cost 10 US$ at the time of this work. Usually the breakdown, caused by the laser, happens on the initial surface of the fiber. This fact allows that only 2 mm may be cut off the fiber to renew the functionability. At first, it feels first like one would cut a hard plastic plate with a blunt knife without any success. But after some movements the glass cladding can be felt as a tougher resistance against the "sapphire proscribe". If this happens only few movements are required to wound the cladding in a way so that the splitting can be performed. A different method of splitting is necessary, other than the classical splitting of glass. One has to take both parts of the fiber in the hands so that the wounded point of the fiber is in the middle, and to apply force to start breaking and to segregate the both ends, as it is shown in the picture 2.10. After usage of the fiber in an experiment resulting in a breakdown, there is no need to cleave a new piece of fiber.

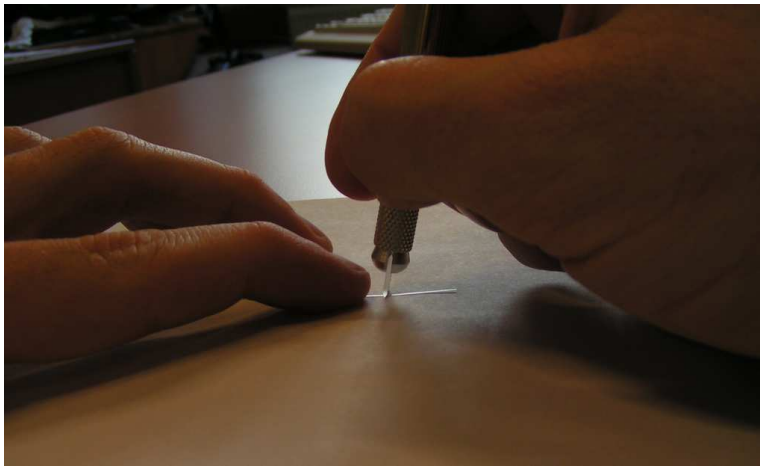

Figure 2.9.: Holding the fiber and starting to scrap the coating. There was no need to remove the coating first. That would only provide a source of damage for the fiber. Moreover the coating was useful for guiding the sapphire proscribe along the wound.

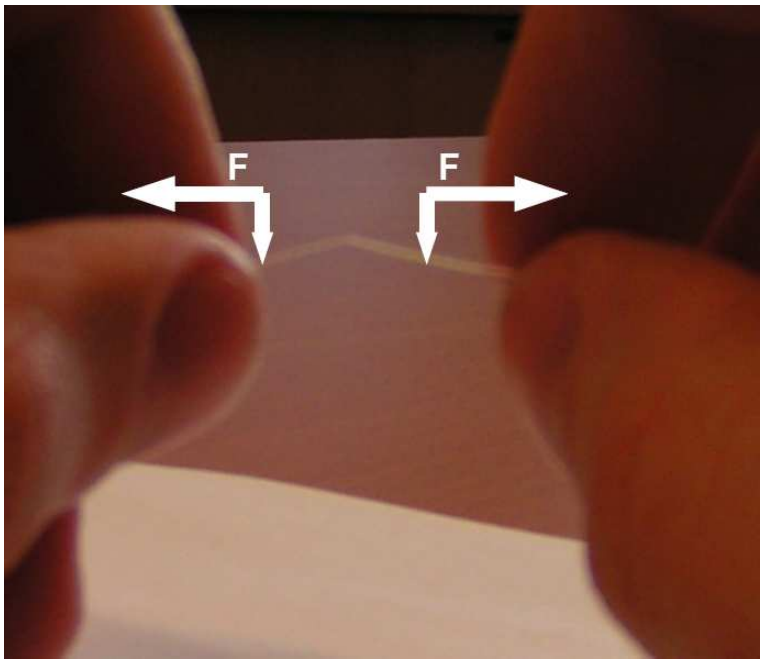

Figure 2.10.: Breaking of the fiber with sketched force application.

2.4.2. Examination of the cleaving result

After the cleaving procedure was successful, the result has to be examined. One can see such result on the figure 2.1 on page 16. As mentioned before, the hollow core has to be free of glass particles for unobstructed transmission. This can be checked with a light optical microscope. There are two aspects to be regarded. First one is the surface of the fiber cut, which has to be as plain as possible and as a matter of course without any glass particles, especially in the core. The second one is the transmisson of the light from the lamp of the light microscope through the fiber. For this examination a microscope is needed, which can feature light from both the top and the bottom. The visualization of the transmission consists of forming a circle in the center of the core filled with a violet colored light (see figure 2.11). The color is defined partially by the design of the fiber for a special wavelength. Both sides of the fiber have to show such behavior.

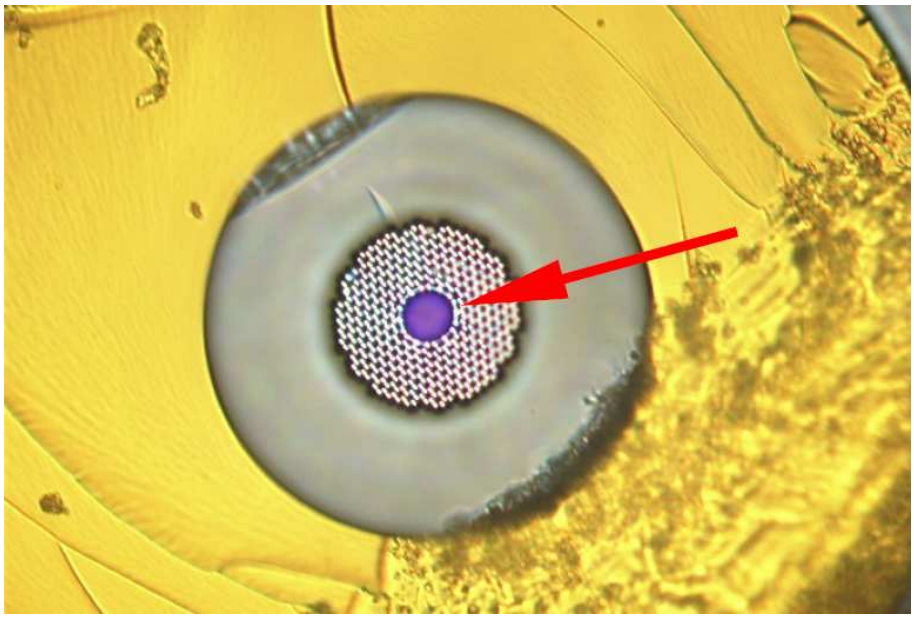

Figure 2.11.: Examination of the cleaving procedure by a light optical microscope. The most important aspect is to obtain the violet spot in the center of the hollow core denoted by the red arrow.

If there is no such violet color filled circle in the core, the transmission is interrupted. The interruption can be caused by a damage, which can be created during the production of the fiber or by incatious handling. After shortening a piece of used fiber, there can still exist a breakdown inside the fiber. This can happen, when the energy accumulates

in some point along the propagation. In this case another new piece of fiber has to be cleaved.

2.5. Coupling

In this subsection the most important action is described. One has to imagine to deposit a laser beam spot of 10 μm size into a core, which is not visible to the naked eye. If using conventional fibers, where the core possesses a refractive index higher than the one of the cladding, the usual method is to do the coupling by finding the highest possible output energy. There is another advantage as well. To visualize, what happens at the front of the fiber, one can consider the reflection coming off the front of the fiber, and then back to the focusing lens and then further to the detector. This method is complicated and consumes much time but provides the most accurate results.

In the case of the PBG fiber with a hollow core, there is no reflection from the core, so that attempting this visualization method would be a waste of time. Although difficult in theory, one has to examine practically the uselessness of such method. At work, first a wrong coupling was established, so that at least some reflection would reach the CCD-detector. The next step was to distinguish the different reflections coming from the window and the focusing lens on the one side and from the fiber on the other side. Not even the selection of the correct reflection was possible, so this type of visualizing was abandoned and regarded as practically useless.

Accurate coupling in the PBG fiber is not achievable by the sole detection of the highest energy or power on the output of the fiber. This can only be considered as a sufficient method in the case of the conventional fiber. The optical energy can in PBG fiber propagate in the periodical structure, which forms a two-dimensional photonic crystal, too. So finding the highest energy is difficult and time inefficient. In the experiments the installation of a CCD-camera together with an energy measurement device proved to be the most efficient combination to visualize and examine the coupling process.

This combination can be integrated on one chip, the so called beam profiler, which simultaneously provides several informations, especially about the beam profile and its energy distribution. However there is also a possibility to do accurate coupling without

an expensive beam profiler. Installing a single webcam with a resolution of at least of 640 x 480 pixels and a removed infrared filter would provide the same information. Those devices use principally the same detection method. The picture of a webcam is monochromatic in comparison with the beam profiler, but gives the information about the energy by displaying the intensity. The best adjustment is just below saturation, because one can see the "envelope" of the energy distribution and with the help of neutral density filters the energy can be lowered. By the gradually lowering of the energy the real energy distribution can be discovered and thus examined if the fundamental mode is actually transferred or some other higher order modes are added. The next figure 2.12 documents these facts.

Figure 2.12.: Gradually attenuated fundamental mode at the output of the fiber. The fundamental mode is characterized by only one intensity peak.

2.5.1. Procedure for coupling

Although using modern devices, such as a 3D micro-positioning stage, the procedure is not trivial. The simplest way to find the best position is to first use a visible continuous laser, for example a green laser pointer. The position adjustment of the collimating lens demands less time and is more precise. In this work the laser pointer was used for fixing the fiber holder in an appropriate distance from the lens, since the micro-positioning stage could not provide enough adjustment travel. Another possible use for the laser pointer was the indication of the beam position while energy measurements for accurate positioning of the measurement device took place. There was only one energy measurement device available, which had to be used alternatively at the input and at the output.

After the adjustment of the components with the help of the laser pointer, the main infrared laser could be activated at a very low energy. For safe use an energy of approximately 10 to 40 μJ per pulse should not be exceeded. The green light lay at another frequency than the Nd:YAG emission, which possesses a wavelength of 1064 nm and unfortunately the focal point changed. The collimating lens had to be readjusted, so that the picture was sharp. Once the picture was sharp, the actual procedure could be started. This procedure consisted of moving the μm screws on the micro-positioning stage and thus finding the focal point. At first, only the screws responsible for the x and y directions (axes) were used. In this manner, the center of the laser beam was sought for, which was identified by a intensive luminous point in the center of the core and was directly associated with the fundamental mode. The stage should not be moved into the direction of propagation (z - axis), because the alignment could not be guaranteed to be perfectly accurate and so the beam might change the direction along the z - axis, which would not be easily noticed. The motion along the z - axis was indicated by intensifying or attenuating of the centered point. If attenuated, the focal plane was already located and one moved away from it, or one was moving into the wrong direction along the z - axis. The motion towards the focusing lens together with an intensification of the fundamental mode represented the approach of the focal plane, at which the bright point was most intensive and there were no other bright spots around.

2.5.2. Interpretation of recorded images related to coupling procedure

The energy measurements could start after the coupling took place. Results of the coupling images taken from the webcam could also be verified by the beam profiler, which gave precise information about the quality of the beam coming from the output of the fiber. In the figure 2.13 there is such a picture captured by the beamprofiler, which was automatically adjusted to the beam and gave information about the beam waist and the intensity distribution in two dimensions and three dimensions.

Other images (figure 2.14 on page 33) taken from the webcam in Russia show two failed and one successful coupling efforts. The left picture was made, because at that moment no fundamental mode could be found and the figure shows the best result at that assigned

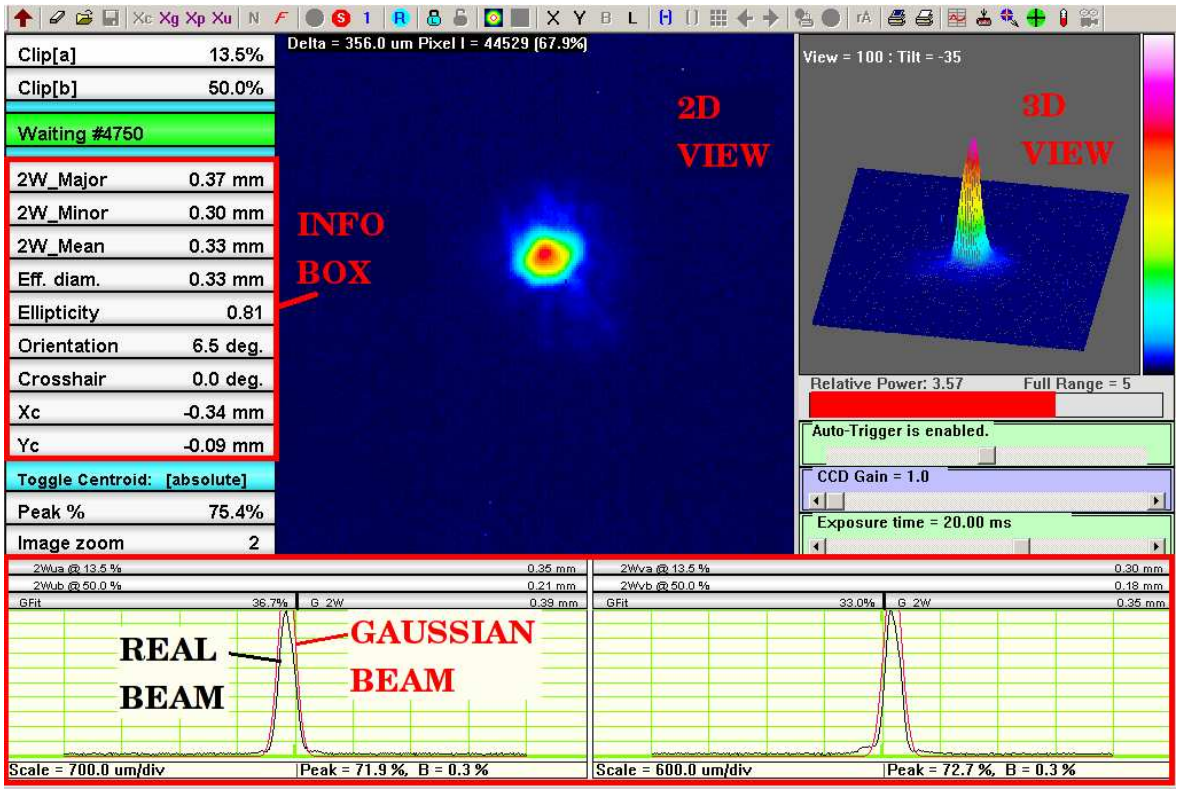

Figure 2.13.: Information provided by the beam profiler. On the left side there is an info box, in the middle a 2D figure and on the right side a 3D beam profile. On the bottom a 2D comparison with a Gaussian beam is provided.

time. The next day the mistake was revealed. It was observed, that using a telescope for fine adjustment during the coupling procedure, especially the motion in z - axis, caused irreversible misalignment to the complete beam propagation path. The recalibration of the propagation path took the entire day. Since that experience the telescope was used only for fine adjustment in x- and y-directions, but no more in z-direction.

2.6. Evacuation of the vacuum chamber

The idea of evacuation is to prevent the formation of plasma in air. Plasma developes in the air when the pulse intensity exceeds the value of 180 GW/cm^2 [8].In this case every matter located in the immediate vicinity is destroyed and turned into plasma. The laser beam is focused forming a spot of 12 μm diameter. To reach the breakdown threshold of air a 6 ns pulse of 1.22 mJ energy is needed. For the purposes of laser ignition in

Figure 2.14.: Left picture shows the output of the fiber for a misaligned beam. The middle picture presents a bad coupling procedure, in which the screws of all directions were moved and no fundamental mode was assured. The right picture displays fully coupled beam into the hollow core of the fiber.

combustion engines a pulse energy of 5 - 10 mJ is required. The natural procedure to prevent plasma formation in the hollow core of the fiber is evacuation. As it is stated later in detail, the maximum non-destructive energy which could be injected into the fiber was 330 μJ in case of using a 6 ns laser pulse. This pulse energy is not sufficient to form plasma. Nevertheless a verification had to be done.

In the beginning of experiments including evacuation only one 2 cm thick aluminum plate was at hand which formed the base plate of the vacuum chamber. Evacuation process consisted of pumping out the air with a conventional vacuum pump and, additionally, by using a turbomolecular pump. The necessity of the additional turbomolecular pump is not for certain. The main reason for it was to assure that also the thin hollow core is evacuated.

In the first experiment a bending of the base plate was observed. Although the micro-positioning stage was placed near the border of the plate, where bending due to the pressure difference should be reduced, the beam deviated 20 μm from the core. To verify that fact a second aluminum plate of 1 cm thickness was constructed, which was completely inside the chamber, so that no pressure dependence should affected the experiment. It was fixed by three thick screws located on the border of the plate to guarantee the independence of the bending from the main plate. After installing the additional plate the deviation explicitly declined. There was still the need to perform a correction, which could be done by adjustingthe mirror which deflected the laser beam into the chamber. In the next figure 2.15, there is a sketch of that additional plate.

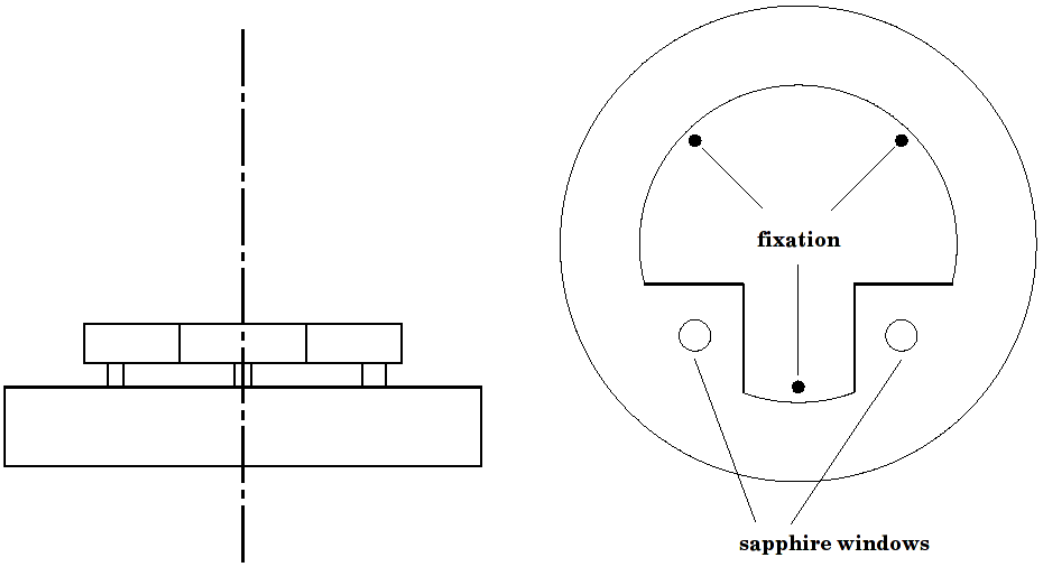

Figure 2.15.: Sketch of the additional plate

It has to be noticed, that the beam deviation from the core was initially considered as a consequence of fiber deflection caused by the air suction of the vacuum pump. In Russia, the components of the vacuum chamber were composed of ordinary steel and the deviation was not so pronounced as it was the case in Austria, where aluminum represented the main material.

Chapter 3.

Results

3.1. Transmission spectrum of the PBG fiber

Due to the special structure of the fiber, forming a two-dimensional photonic crystal, a certain number of frequencies can be determined, which experience constructive interferences in the core.The hollow core diameter and the interhole spacing Λ are mainly responsible for this selection. In some respect, this can be ascribed to the existance of band gaps, in which light is not allowed to propagate. Thus, light with a certain frequency can only be guided in the hollow core. According to this concept, also a transmission spectrum should show such a behavior. The transmission spectrum of the hollow core PBG fiber was obtained by a spectrometer "Ocean Optics", that could only provide accurate detection of spectrum range between 450 nm and 950 nm. Nevertheless, in the figure 3.1 on page 36, one can see a high peak near 700 nm and several other peaks aside, which indicate the gaps and thus the wavelength (or frequency) selection. On the picture one interesting aspect appeared. It was expected, that using a design of the fiber for wavelength of 1064 nm, where the highest peak should be situated, one peak would appear as well at a half wavelength of 532 nm (doubled frequency of the main emission by a non-linear crystal), but the opposite occured and at that position a high attenuation of the light took place. This can be explained by following: At the wavelength of 532 nm the two-dimensional photonic crystal structure in the fiber cladding does not allow the propagation of light in the hollow core, because there is no full photonic band gap. In the peak areas, the attenuation should be minimal. Figure 3.2 shows the attenuation

profile for the area covering the desired wavelength of 1064 nm. For some interval the attenuation stays at its minimum of approximately 80 dB/km[1] and then rises to 140 dB/km just 60 nm away from the center. A 60dB jump means a reduction of the energy by the factor 1,000.000 to its previous value.

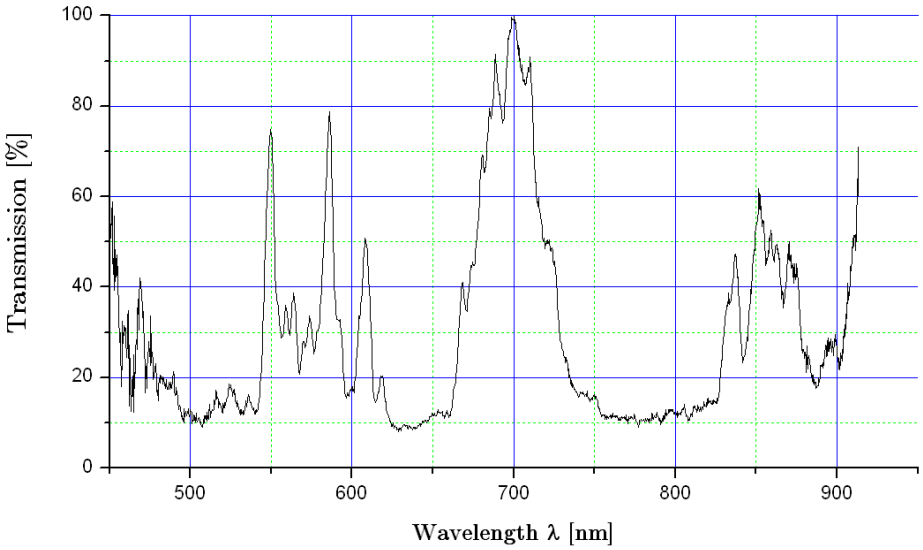

Figure 3.1.: Transmission spectrum of the PBG fiber. At the wavelength of 700 nm there is a high peak which represents the existance of full photonic band gap and at which the attenuation has a minimum. On both sides several other peaks denote allowed high transmitance in the hollow core. Due to the limited range of the spectrometer, the spectrum at 1064 nm could not be observed.

3.2. M^2 of the employed lasers

As well as a part of the project "Laser Ignition", for ensuring high quality coupling results it seemed necessary to measure the M^2 parameter of both lasers "Quantel Brilliant[2]" and "Litron[3]". In practice, Quantel ignited gas mixtures better than Litron. These experiments were a welcome opportunity to determine the reasons for that behavior. For M^2-measurements the following setup (figure 3.3) was established.

[1] dB means "decibel" and it is a logarithmic value. Details are explained in appendix A
[2] www.quantel.fr/uk/scien/brilliant.htm
[3] www.litronlasers.com/index.html

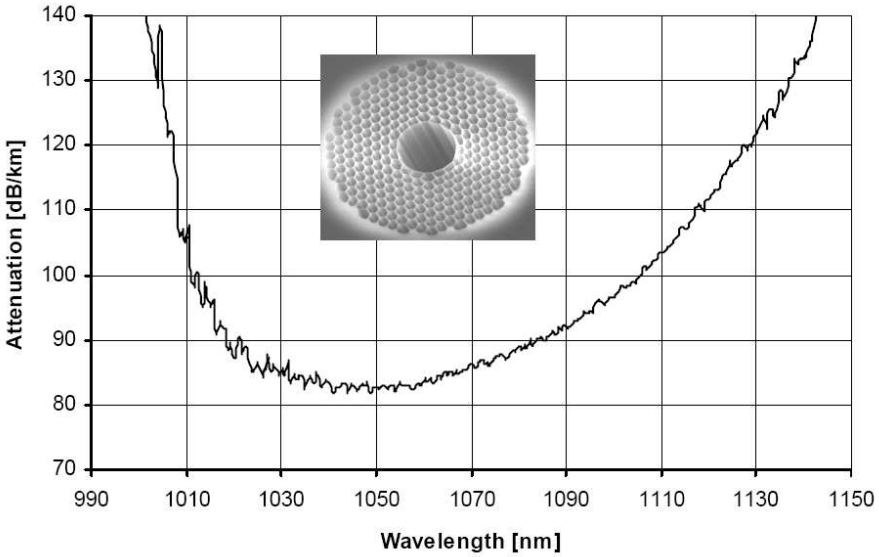

Figure 3.2.: Attenuation profile in the area around the desired wavelength of 1064 nm, where the attenuation reached its global minimum. This global minimum depends on the hollow core diameter and the interhole spacing Λ in the two-dimensional photonic crystal forming the cladding around the core.

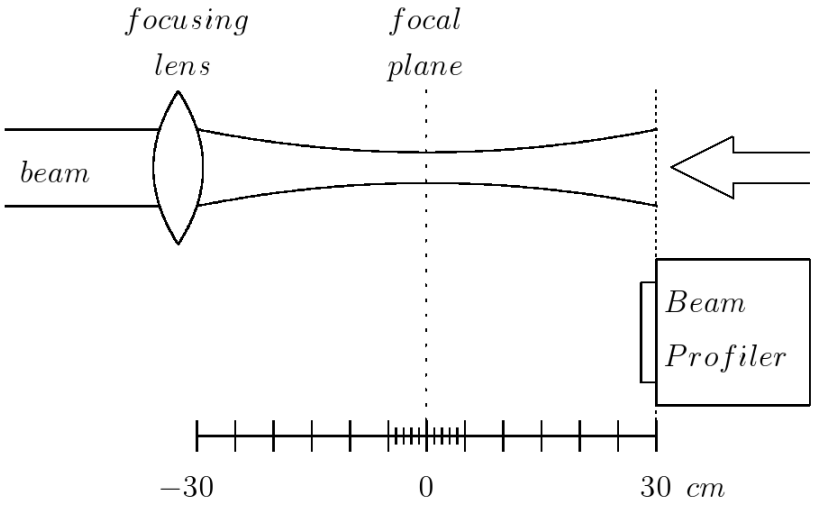

Figure 3.3.: Sketch of the M^2-mesurement setup

For the focusing of the laser beam, 60 cm behind the main laser output a conventional lens with a focal length of 300 mm was installed, which should be sufficient for providing a large enough area around the focal plane to be able to capture more than adequate information about the beam diameter. With the first step it was assured that the laser beam hit the centre of the lens and then it was attenuated, so that the beam profiler could not be destroyed by the intensity in the focal point. In the second step the mentioned focal point was determined by placing the beam profiler in the forecasted focal point and moving it along the propagation axis to find the intensity maximum. After finding the focal point, informations about the mean beam diameter were gathered in primarily 1 cm intervals around the focal plane and then in 5 cm intervals as depicted in figure 3.3.

To finally calculate M^2, two methods were used for computation, which are explained in detail in section "Quality of the laser beam and M^2" on page 10. The first method was termed "divergency of the beam", because faster divergence by the factor M^2 was considered (item a)) and the second one was denoted as "focusability", because the enlargement of the focused beam waist by M^2 was regarded (item b)).

3.2.1. Quantel Brilliant

Quantel Brilliant is supposed to be the best laser dedicated to laser ignition among all lasers at the university. The focal point was found in a distance of 31 cm, which means 1 cm in addition to the specified focal length of the focusing lens. This is due to the fact that Quantel possesses a beam diameter of 5.6 mm and nearly fully filled the lens aperture. The diameter of the beam in the focal plane decreased to 0.11 mm and showed nearly perfect Gaussian profile. 26 cm behind the focal plane again the same profile was established, called "flat top". From the information about the mean diameter of the beam, gathered from the beam profiler, M^2 could be calculated (resulting in $M^2 = 1.42$) and so the real beam could be compared to the ideal Gaussian beam in two respects. As mentioned in chapter 1.4.1, one can consider a real beam which diverges faster than the Gaussian beam for a given waist or the consideration can be based upon a real beam having the same divergence as the Gaussian beam but a different waist. Both considerations are depicted in figure 3.4. In the figure 3.5 on page 40 the profile

in the focal plane is shown and in the next figure 3.6 the profile of the laser beam in 26 cm distance from the focal plane is presented.

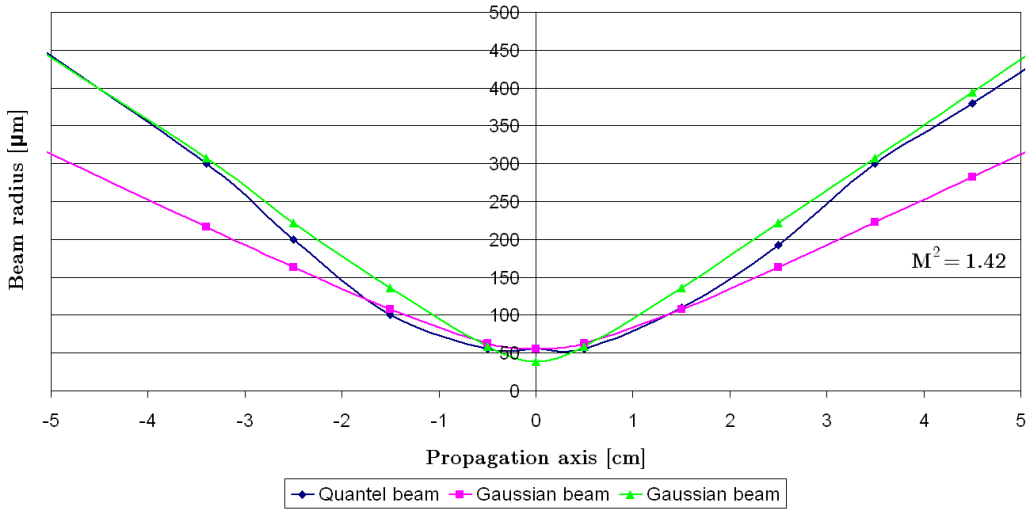

Figure 3.4.: Comparison of the beam produced by the Quantel laser with Gaussian beams. The blue trace is produced by the real laser beam. Compared to the magenta trace, the beams have the same waist but different divergence. The green Gaussian beam possesses the same divergence but a smaller waist.

3.2.2. Litron

The output beam of this laser was tighter than the one from Quantel. The diameter was 1.8 mm, measured 60 cm behind the output. This diameter increased to a value of 3.2 mm in 2 m distance and it was expected, that M^2 would be higher than the one of the Quantel laser, which would explain its better functionality in ignition experiments. But only results of the measurements could uncover that fact. Due to the smaller diameter of the laser beam, the aperture of the focusing lens was not fully filled, which caused a greater spot in the focal plane, namely 0.35 mm in diameter. The procedure of gathering information about the mean diameter was the same as in the case of Quantel and described at the beginning of this section (see also figure 3.3 on page 37). Unlike the prediction that Litron would possess worse beam properties than Quantel, the result of the computation showed that Litron produced a real beam characterized with a M^2 of 1.54, which represented a quality beam nearly as high as the one emitted by Quantel. The following figures substantiate those facts. Figure 3.7 represents the comparison of

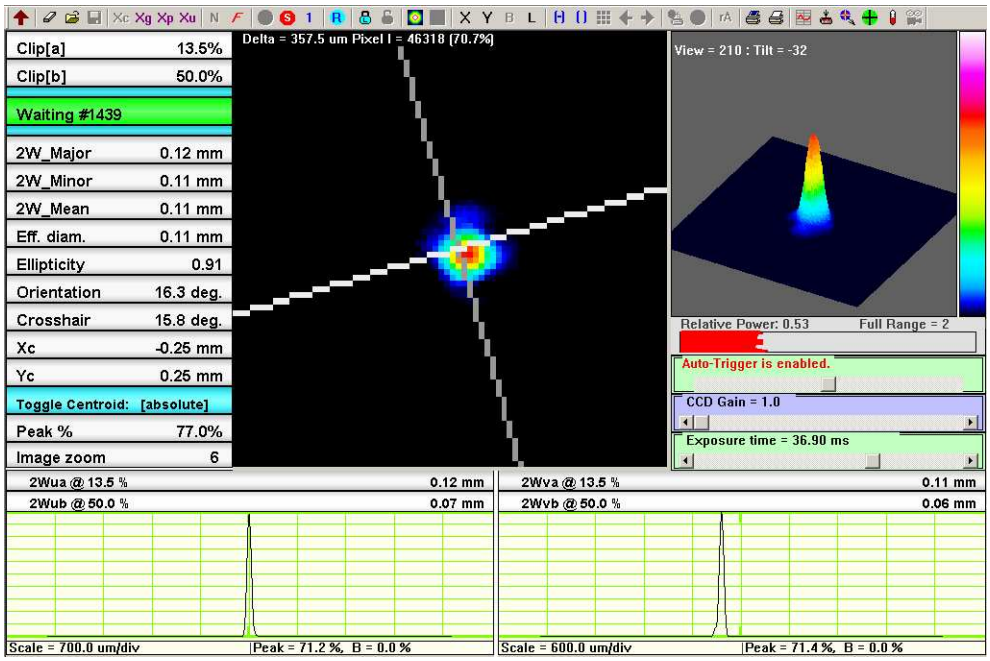

Figure 3.5.: Recorded profile of the beam produced by Quantel in the focal plane using a 6-fold zoom.

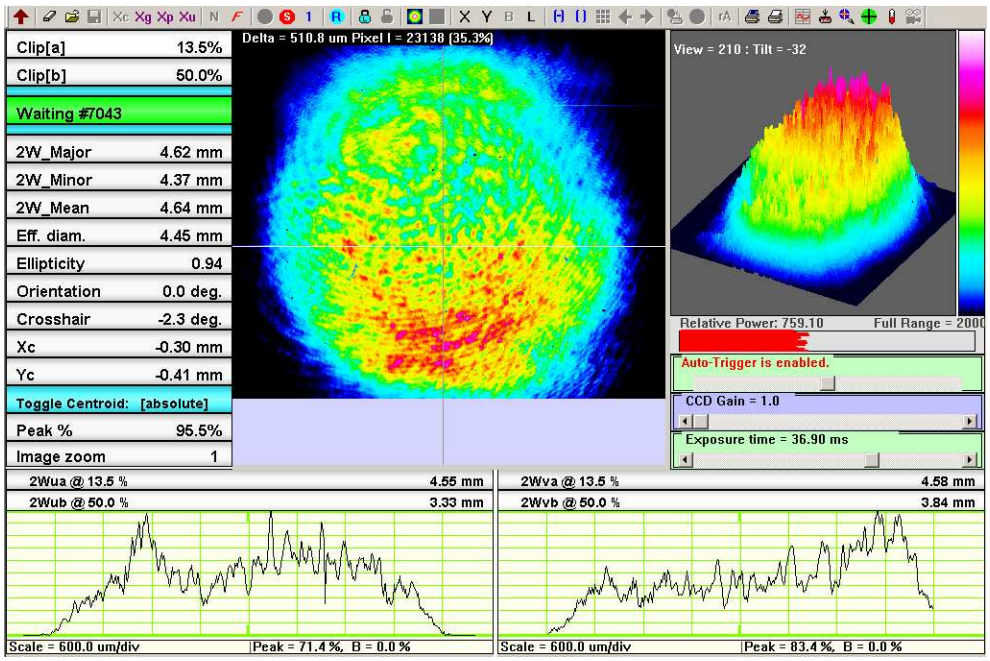

Figure 3.6.: Recorded profile of the beam produced by Quantel in 26 cm distance from the focal plane.

the real beam with the Gaussian beams and the figures 3.8 and 3.9 on page 42 and 42 show the intensity profiles and give information about the diameters in the focal plane and in 30 cm distance from the focal plane.

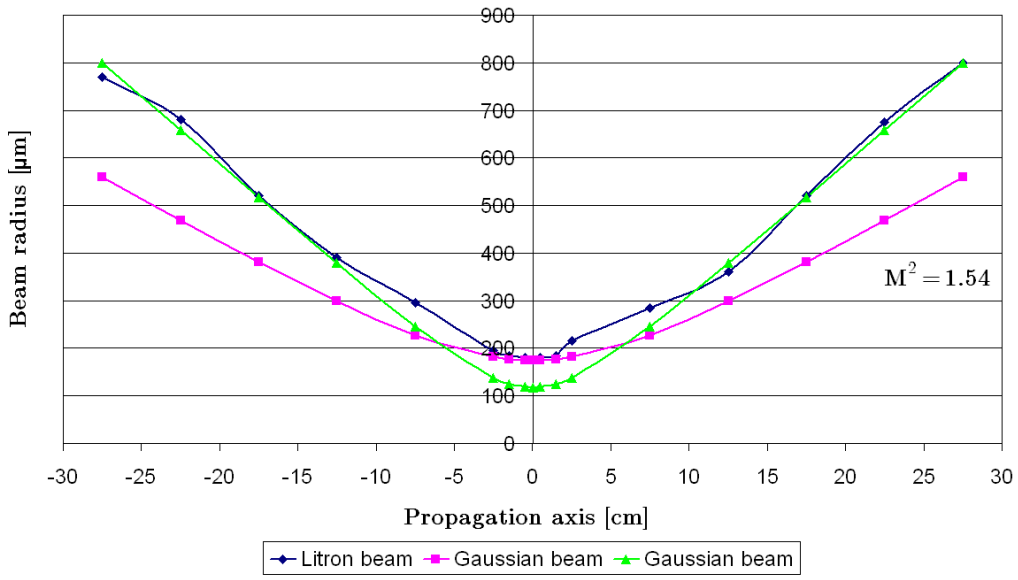

Figure 3.7.: Comparison of the beam produced by the Litron laser with Gaussian beams. The blue trace is produced by the real laser beam. Compared to the magenta trace, the beams have the same waist but different divergence. The green Gaussian beam possesses the same divergence but a smaller waist.

3.2.3. Summary

The results were computed and plotted in Microsoft Excel, that means that the "Second moment method" was not applied for the calculation. This happened due to the lack of a software module that would provide the correct and complete data for such "Second moment method" calculation. That was the reason why the mean values of the diameter were taken for the calculation and why M_x and M_y were not distinguished. For the sake of completeness, it was interesting to know the quality of both laser beams and motivating to find out if Quantel provides a better beam quality than Litron. M^2 of approximately 1.5 stands for high quality laser beams, which can be used in experiments with the PBG fiber without suffering from high energy losses in the coupling process.

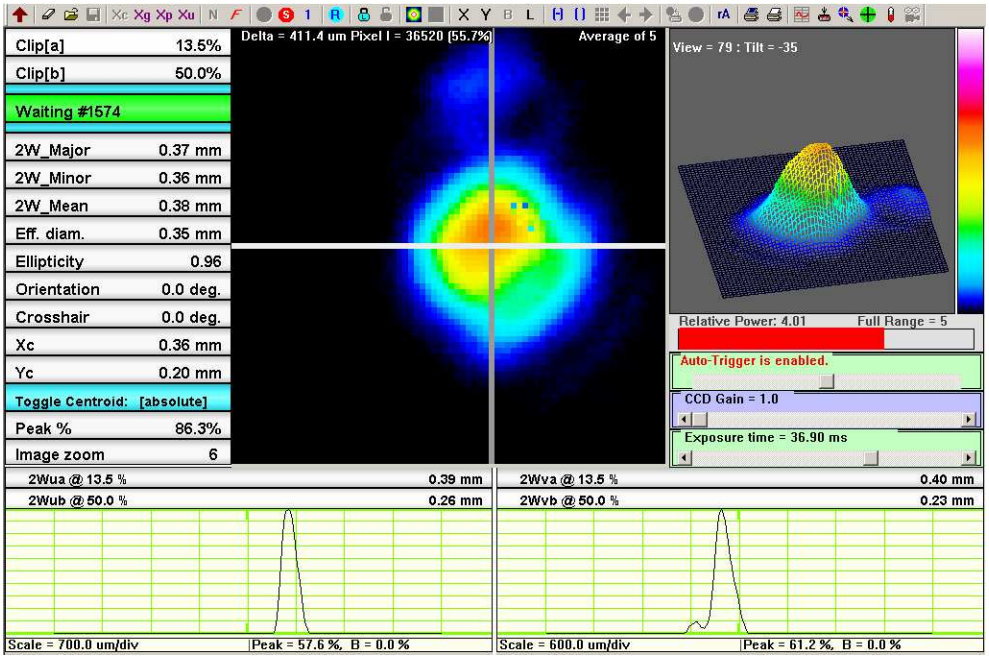

Figure 3.8.: Captured beam profile produced by Litron in the focal plane using a zoom step of 6 times.

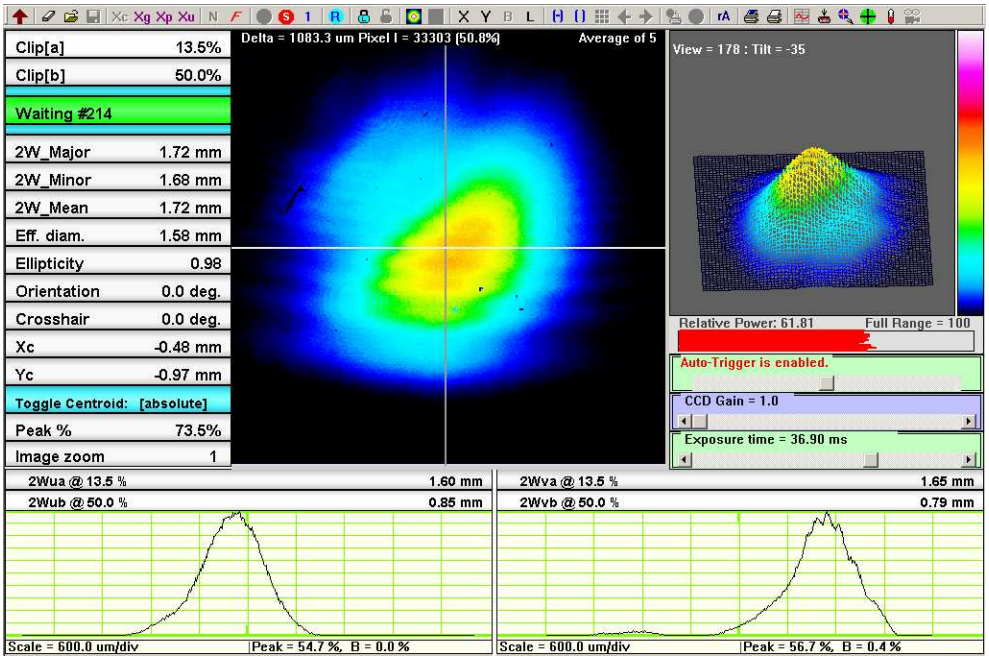

Figure 3.9.: Captured beam profile produced by Litron in 30 cm distance from the focal plane.

With the help of such measurements one can verify the fact that adjusting the laser at one point to resemble a Gaussian beam does not mean that the laser beam has the same properties along the complete path, which is clearly observable and recognizable in the figures. Additionally, Q-switched lasers suffer from poorer quality of the emitted beam than mode-locked lasers. That is the reason why apertures inside the cavity are used to cut off the higher order modes, that are thus not gained. In case of Litron a 1.6 mm aperture was employed.

3.3. Efficiency and breakdown measurements

This section is divided into two subsections providing the results gathered in Russia first, and then the results obtained in Austria. There are more reasons for this division. On one side, lasers with different properties were applied for the experiments and on the other side, different coupling methods were used.

In Russia the Nd:YAG laser produced laser pulses with a duration of approximately 10 ns, which was nearly twice as much as the duration of the laser pulse emitted by the laser used for extensive experiments in Austria that was Litron. The repetition rate of the Russian laser was set to 2 Hz while Litron's repetition rate was adjustable from 1 Hz up to 50 Hz.

In Russia, windows made of glass and microscope objectives were installed, whereas in Austria sapphire windows and aspherical lenses were available. Thus, different losses of the windows, or objectives respectively had to be taken into account. In Russia, the windows caused energy losses of 8 % and microscope objectives attenuated the energy by 18 %, whereas in Austria only the sapphire windows generated noticeable losses of 15 %.

3.3.1. Results obtained in Russia

The experiments in Russia were performed in the Laboratory of Photonics and Nonlinear Spectroscopy on the chair of General Physics and Wave Processes. Based on long time experience with micro-structured fibers, such as e.g. PBG fibers, the decision for

the focusing microscope objective was made to use magnifications 10x and 20x. The objective with 20x magnification appeared to be the best solution and was used for the forthcoming experiments. It produced a focal spot with the diameter of 14 μm and the numerical aperture was matched to the one of the fiber.

The first step was to measure the transmission spectrum, which is described in detail in chapter 4.1 on page 35. Then experiments with the visible 532 nm laser emission were performed to determine the behavior during the coupling process and to gain experience in handling this type of the hollow core PBG fiber. Using the Nd:YAG laser emitting at a wavelength of 1064 nm, the following results were achieved. In figure 3.10, the maximum pulse energy delivered at the output of the fiber is compared to the input pulse energy under atmospheric air pressure (1 bar), which was transmitted safely and reliably through the fiber without damage. In the figure, losses of the windows and the microscope objectives are already extracted.

In order to examine the breakdown threshold, which was expected to be also dependent on the pressure, experiments in the (vacuum) chamber took place. The pressure was gradually adjusted. The low pressure limit introduced by the vacuum pump was at pressure of 450 mbar. To receive informations about the pressure dependency of the breakdown threshold energy, a pressure of 750 mbar was established, at which the highest threshold was found in the middle of the range of the pressure interval. This result is shown in the figure 3.10.

An extraordinary result could be obtained at the lowest pressure setting of 450 mbar. The barrier of 1 mJ input pulse energy was overcome and now this amount of energy could be injected into the fiber. The value of 1025.98 μJ gave a rise to the idea that pressure settings can influence the breakdown threshold of the fiber. The result is plotted in the figure 3.10 together with other results obtained at 1 bar and 750 mbar. The discussion about this remarkable outcome of the experiment is conducted in the conclusion, in the section 3.4 on page 51. termed Conclusion. It is necessary to notice, that this result was obtained only once, which on the one side indicates that it was possible to achieve such result but on the other side it is necessary to repeat such experiment to prove that result. Unfortunately, in forthcoming experiments such result could not be achieved again.

The aspect of the energy efficiency, or in other words, the ratio of the output pulse

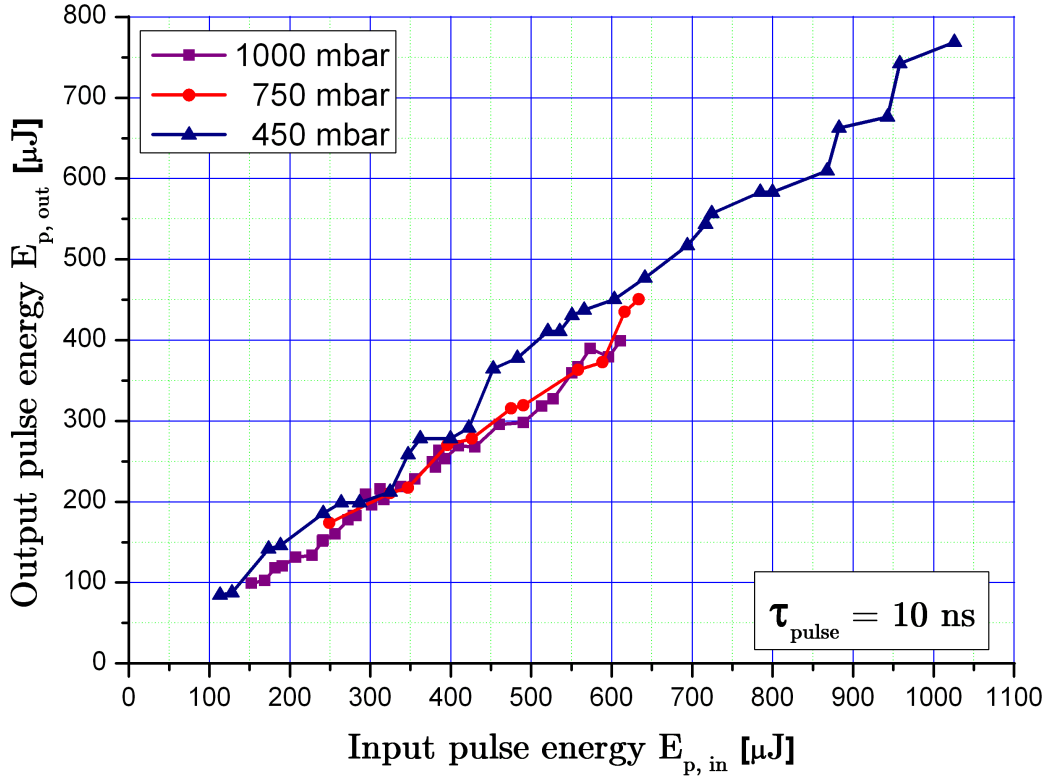

Figure 3.10.: The output pulse energy versus the input pulse energy established at a pressure of 1 bar (violet trace), 750 mbar (red trace) and 450 mbar (blue trace). At 450 mbar, the input pulse energy overcame the value of 1 mJ, which marked the highest obtained breakdown threshold energy for this type of micro-structured fiber.

energy E_{out} to the input pulse energy E_{in} obtained at different stages of experiments is introduced to find out if the coupling process was successfully achieved and at which conditions the best result could be accomplished. In the figure 3.11 the mean efficiency and the maximum efficiency in each case is depicted. It is noticeable, that the maximum value is 81.74 % achieved in the experiment performed at 450 mbar pressure, when also the highest breakdown threshold was recorded.

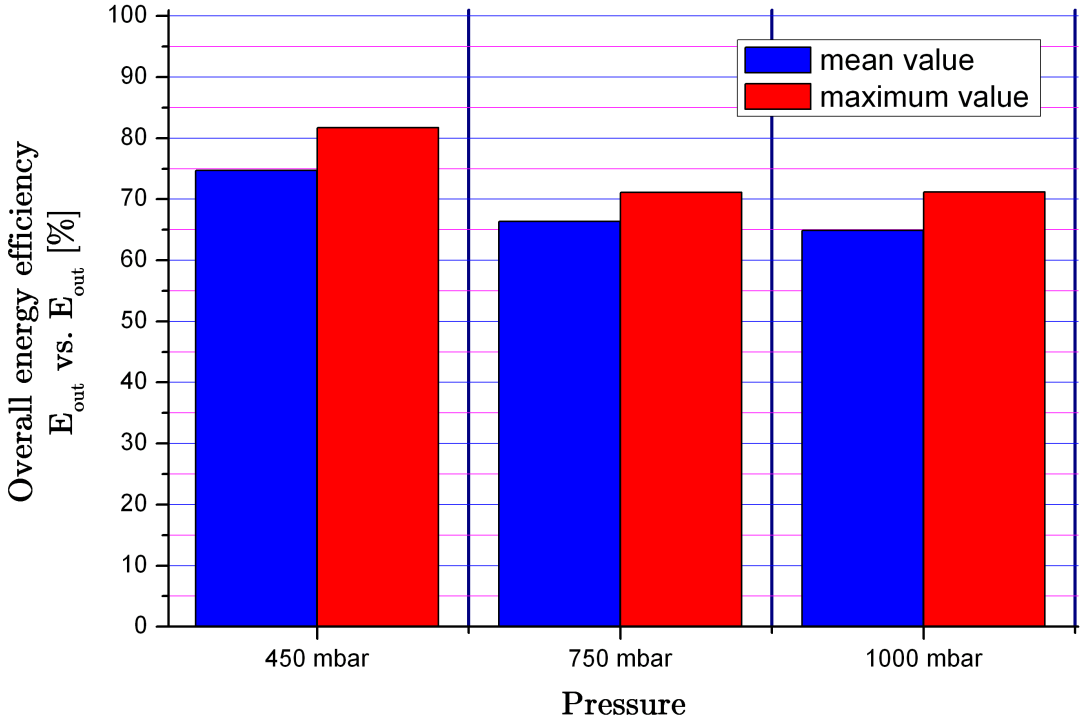

Figure 3.11.: The mean and the maximum ratio of E_{out} to E_{in}. The maximum value of approximately 82 % was obtained in the experiment with the highest achieved breakdown threshold.

3.3.2. Results obtained in Austria

With other equipment than in Russia, in Austria there was the motivation at least to repeat the promising results. Promising in a way, so that the rising breakdown threshold with the dropping pressure obtained in Russia could be overcome due to an additionally installed turbomolecular pump, allowing to create pressure of around 0.1 mbar. Would the behavior continue in the way as it did in Russia, the maximum pulse energy of the laser would not be high enough to initiate the breakdown of the air and thus of the fiber. The results achieved in Austria in contrast show a different behavior. It was found that there is no dependence of breakdown thresholds of the fiber on the pressure, which represented a negative result in comparison to that achieved in Russia. The Austrian results thus were a supplement to the results in Russia. The target aimed in Austria was to form plasma with approximately 10 mJ coming out at the output of the fiber, situated inside of the evacuated chamber, by refocusing the beam with the help of a lens.

In order to provide conditions as they prevail in combustion engines, a repetition rate of 12.5 Hz was set. To simulate approximately the same conditions according to those in Russia also experiments at a repetition rate of 2 Hz were examined. In the experiments, it was observed that no difference appeared between 2 Hz and 12.5 Hz, which is rather obvious as no thermal effects are assumed to play a role. Thus, all breakdowns were caused by the peak power of the single pulse and no thermal breakdown showed up. The figure 3.12 shows the results achieved with an installed focusing lens with a focal length of 11 mm and 7.5 mm under air pressure (1 bar).

266.67 μJ was the first highest threshold energy achieved in the laboratory, which led to the fiber damage. The aspherical lens with a focal length of 11 mm provided the best overall energy efficiency (maximum ratio of the output pulse energy E_{out} to the input pulse energy E_{in}) due to having a lower numerical aperture (NA) than the fiber and thus the lowest energy losses appeared in the coupling process as it can be considered in the figure 3.14 on page 50. On the other side, the lens produced a focal spot with a diameter of 17 μm, which was greater than the diameter of the hollow core and in this manner a significant amount of energy touched the wall of the hollow core. Later on, it was determined that using this focusing lens, the lowest breakdown thresholds were observed. The figure 3.13 displays the result achieved using the focusing lenses with a

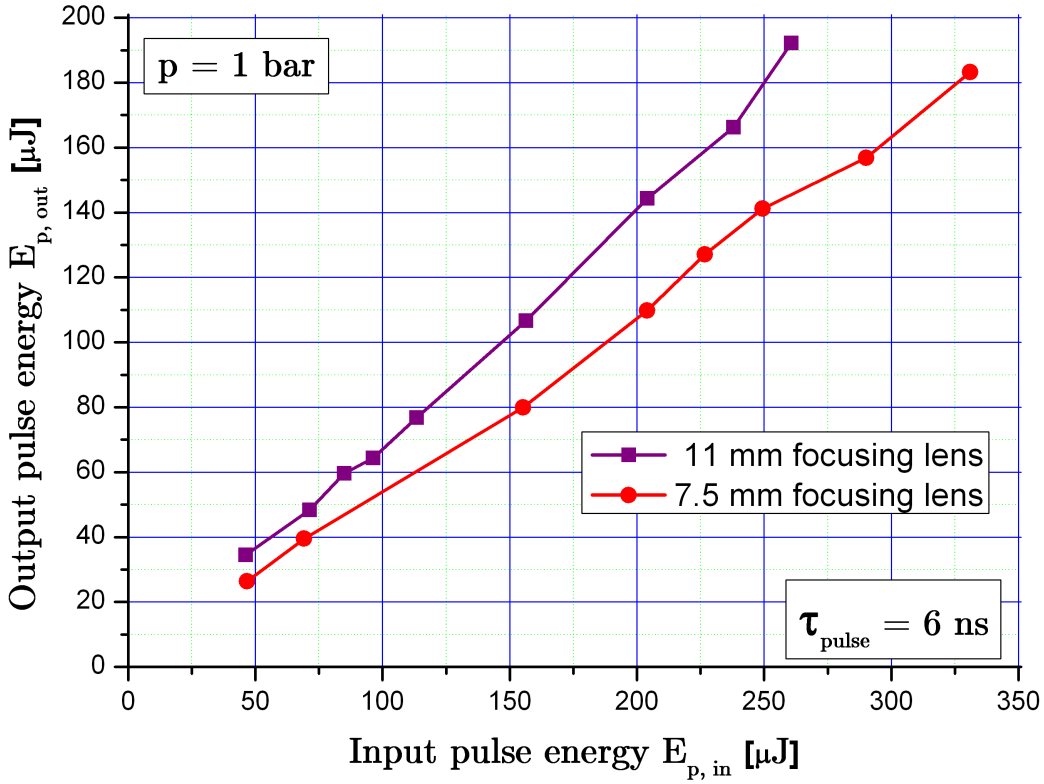

Figure 3.12.: The output pulse energy versus the input pulse energy using focusing lens with a focal length of 11 mm (violet trace) and 7.5 mm (red trace) at air pressure (1 bar). τ_{pulse} denoting the laser pulse duration of 6 ns.

focal length of 11 mm, 7.5 mm and 4.5 mm under 0.1 mbar pressure.

Because a focusing lens with a focal length of 11 mm did not provide sufficient tight focusing, another focusing lens with a focal length of 7.5 mm was chosen. Again there was the expectation that with this lens creating a spot having the diameter of 12 μm, a higher breakdown threshold could be achieved. If the formed plasma in the air leads to a breakdown of the fiber, the evacuation would allow to perform the experiment without plasma formation. Fortunately, the breakdown threshold rose a little bit to 330.93 μJ under atmospheric air pressure (1 bar), which denoted the best achieved performance. This result can be regarded in the figure 3.12 on page 48.

Even evacuation could not provide an improvement. The maximum input pulse energy

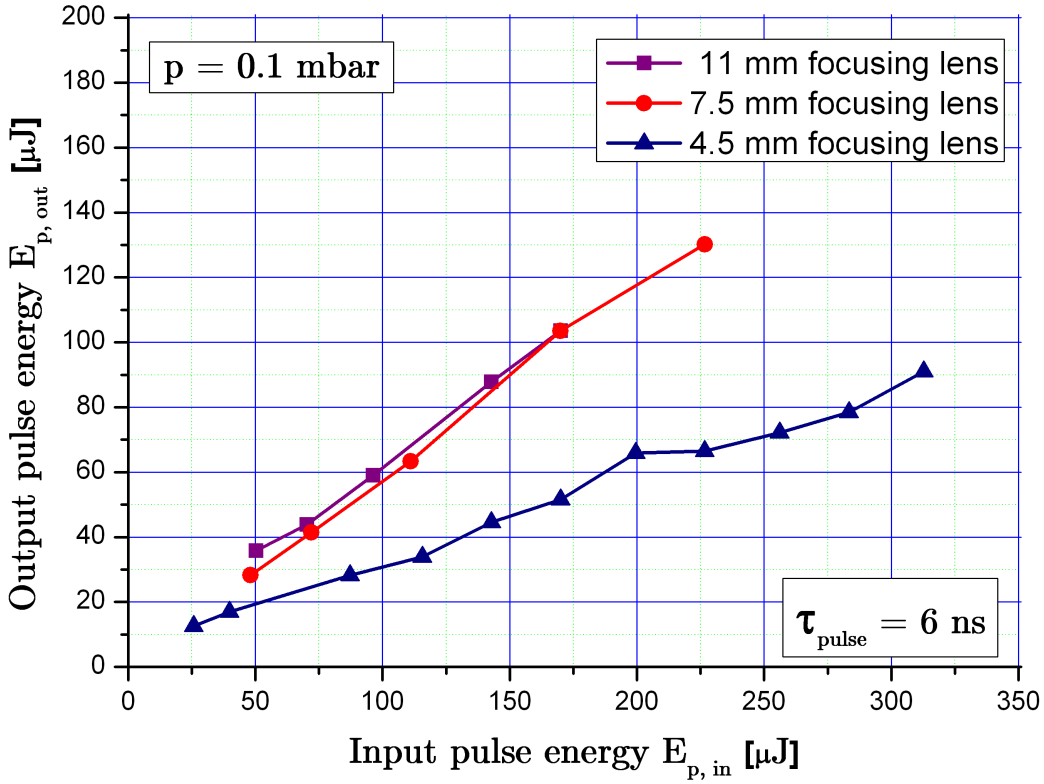

Figure 3.13.: The output pulse energy versus the input pulse energy using focusing lens with a focal length of 11 mm (violet trace), 7.5 mm (red trace) and 4.5 mm (blue trace). τ_{pulse} denoting the laser pulse duration of 6 ns.

decreased in this case from 330.93 μJ to 226.67 μJ. This energy value was the usual and thus most common energy value during all experiments, at which still no breakdown of the fiber appeared. Due to a higher NA than the one of the fiber, the overall energy efficiency remained under 60 % (see figure 3.14 on page 50). In the figure 3.13 the output pulse energy versus input pulse energy is plotted showing results under 0.1 mbar pressure.

To prove the fact that sufficient focusing was provided by the lens with the focal length of 7.5 mm another experiment took place inserting a focusing lens with a focal length of 4.5 mm and NA of 0.55. As mentioned before regarding the most common laser pulse energy value, which did not lead to breakdown of the fiber stated at approximately 230 μJ, also in this experiment the breakdown threshold did not overcome the value of 312.8

μJ. In this case the experiment was realized under the pressure of 0.1 mbar and the figure 3.13 emphasizes that fact.

As it can be recognized, the energy efficiency suffered highly due to the high difference between the NA of the lens and the fiber. Only one third of the energy was transmitted, whereas the rest was lost mostly in the coupling process in the case of the 4.5 mm focusing lens. For the sake of completeness, the figure 3.14 shows the overall energy efficiency achieved all over experiments. It can be seen on this figure that the best performance was obtained by using the focusing lense with a focal length of 11 mm. In contrast to that, in this case also the lowest breakdown thresholds were observed in air as well as under 0.1 mbar pressure. Compared to the other focusing lenses with a focal length of 7.5 mm and 4.5 mm, the pulse energy delivered at the output was the highest under air pressure, namely 192.16 μJ. In the case of the 7.5 mm focusing lens (achieving the highest breakdown threshold) it was only 183.22 μJ.

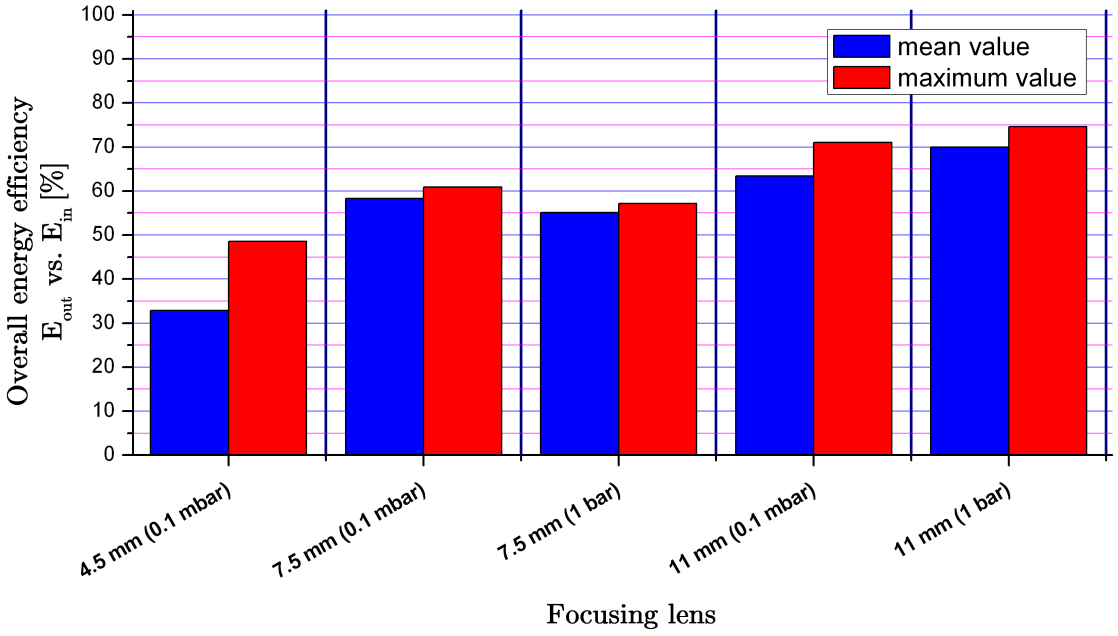

Figure 3.14.: The mean and maximum ratio of E_{out} to E_{in}. Different focusing lenses (4.5 mm, 7.5 mm and 11 mm) were used at different pressure settings (0.1 mbar and 1 bar). The highest value of 74.63 % was obtained in the experiment using the focusing lens with a focal length of 11 mm under air pressure.

3.4. Conclusion and outlook

Regarding all the results, it can be concluded that PBG fiber with hollow core diameter of 15 μm designed for 1064 nm emission cannot transmit the desired amount of pulse energy needed for laser ignition purpose, stated at 10 mJ at a pulse duration of 6 ns. The highest pulse energy successfully injected into the fiber during the experiments carried out at the Lomonosov Moscow State University was a little bit more than 1 mJ in the case of 10 ns pulse duration. After the breakdown occured at higher pulse energies, the fiber was examined and prepared to be shortened again for the next experiment. After cutting off a piece of the front of the fiber in this case it was observed for the first time that no light came through the hollow core of the remaining fiber piece during the examination of the cleaving result under the light optical microscope. This approved the assumption that the breakdown could appear at every point along the fiber, and not only at the input facet. The same behavior of the fiber was noticed in corresponding experiments in Austria as well. Applying approximately 2 mJ of pulse energy, the breakdown happened not only on the input facet of the fiber, where usually breakdowns at lower energies were observed, but also at some point inside the hollow core channel. This in turn demonstrates that in case of no destruction at the input facet, breakdown can also happen inside the fiber, which means that the fiber cannot reliably transmit more energy than observed in the experiments.

Considering the observed dependency of the breakdown thresholds on the pressure in Russia, it can be assumed that the dependency was actually not on the applied pressure but on the achieved energy efficiency (E_{out}/E_{in}). In Austria, the only dependency observed was on the NA of the focusing lens. The threshold rose because the focal spot diameter was scaled down by the shortening of the focal distance.

Comparing the results with those achieved with conventional fibers, there is only one conclusion. The intensity, which can be applied to the conventional optical waveguides, is limited to 1 GW/cm^2 by the manufacturer. The breakdown of such step index fibers was observed at an intensity of 2 GW/cm^2 in [11] compared to a highest intensity transmitted through the PBG fiber of 66.62 GW/cm^2, which is 33.3 times as much. The longer the laser pulse duration lasts the higher an energy per pulse can be transmitted. Although this may sound trivial, no proportionality of the peak energies could be found between the breakdown thresholds in Russia using a 10 ns laser pulse duration and those

recorded in Austria using a 6 ns laser pulse duration. One could simply assume that in case of double pulse duration, the breakdown threshold would double in the same way. In the case of 6 ns laser pulse duration, the calculated threshold intensity result equals only to 55 GW/cm^2. This, however, is another prove that this fiber is only of limited applicability for the laser ignition purposes.

In the group of scientists dealing with the topic of laser ignition of engines, a new idea arose. The suggestion was to use optical energy from a laser on the one side and simultaneously an electrical spark on the other side. The additional electrical spark would help to reduce the minimum laser pulse energy required to form a plasma in the combustion engine. First tests showed a significant reduction of the required minimum pulse energy of the laser to a value of approximately 200 μJ, which represents an amount of energy that could reliably be transmitted through the hollow core PBG fiber used in the experiments.

Using hollow core PBG fibers to transmit optical energy to engines requires precise focusing and accurate coupling, which is difficult to provide in real conditions and expensive to realize. One approach for further development could be a larger hollow core, which would decrease the peak intensity and thus simultaneously increase the breakdown threshold. The highest peak power applied to the fiber was nearly 100 GW which equals to an intensity of 58 GW/cm^2 at a diameter of 15 μm. In the case of a 20 μm core diameter (a 33 % increase) the critical intensity would decrease to 32.63 GW/cm^2, which is a little more than one half of the previous intensity. The probability for forming plasma in the air inside the core would also decrease. It remains to determine, if such a fiber which can deliver a single mode beam at the output, could be usefully employed in practice.

Bibliography

[1] Al-Janabi, A. H. . E. Wintner: *High power laser transmission through photonic band gap fibres*. Laser Physics Letters, . 1–4, feb 2004.

[2] Arriaga, J., J. C. Knight . P. S. Russell: *Modelling photonic crystal fibres*. Physica E, 17:440–442, 2003.

[3] Arriaga, J. . B. Meneses: *Band structure for the cladding of a hollow core photonic crystal fibre*. Revista Mexicana de Fisica, 49(4):335–337, feb 2003.

[4] Broeng, J., S. E. Barkou, T. Sondergaard . A. Bjarklev: *Analysis of air-guiding photonic bandgap fibers*. Optics Letters, 25(2):96–98, jan 2000.

[5] Broeng, J., T. Sondergaard, S. E. Barkou, P. M. Barbeito . A. Bjarklev: *Waveguidance by the photonic bandgap effect in optical fibres*. Pure Applied Optics, 37:477–482, mar 1999.

[6] Buczynski, R.: *Photonic Crystal Fibers*. Acta Physica Polonica A, 106(2):141–167, 2004.

[7] Chan, S. H.: *Transport Phenomena in Combustion*, jul 1995.

[8] Chylek, P., M. A. Jarzembski, V. Srivastava . R. G. Pinnick: *Pressure dependence of the laser-induced breakdown thresholds of gases and droplets*. Applied Optics, 29(15):2303–2063, may 1990.

[9] Du, D., X. Liu, G. Korn, J. Squier . G. Mourou: *Laser-induced breakdown by impact ionization in SiO_2 with pulse widths from 7 ns to 150 fs*. Applied Physics Letters, 64(23):3071–3073, mar 1994.

[10] Geckeler, S.: *Lichtwellenleiter für die optische Nachrichtenübertragung.* Springer-Verlag, 3 ., 1990.

[11] Gilber, R.: *Ausbreitung von 1 µm ns-Impulsen über optische Fasern.* master thesis, 2003.

[12] Inc., P. P.: *www.fibertools.com/Products/Scribes/Scribes.htm.*

[13] Johnston, T. F.: *Beam propagation (M^2 measurement made as easy as it gets: the four-cuts method.* Applied Optics, 37(21):4840–4850, jul 1998.

[14] Knight, J. C., T. A. Birks, R. F. Cregan, P. S. Russel . J. P. Sandro: *Photonic crystals as optical fibres - physics and applications.* Optical Materials, 11:143–151, jan 1999.

[15] Konorov, S. O., A. B. Fedotov, O. A. Kolevatova, V. I. Beloglazov, N. B. Skibina, A. V. Shcherbakov, E. Wintner . A. M. Zheltikov: *Laser breakdown with millijoule trains of picosecond pulses transmitted through a hollow-core photonic-crystal fibre.* Institute of Physics Publishing, 36:1–7, march 2003.

[16] Konorov, S. O., V. P. Mitrokhin, A. B. Fedotov, D. A. Sidorov-Biryukov, V. I. Beloglazov, N. B. Skibina, E. Wintner, M. Scalora . A. M. Zheltikov: *Hollow-core photonic-crystal fibres for laser dentistry.* Institute of Physics Publishing, 49(1):1359–1368, feb 2004.

[17] Leung, K. M. . Y. F. Liu: *Photon band structures: The plane-wave method.* Physical Review B, 41(14):10188–10190, jan 1990.

[18] Magerl, G.: *Mikrowellenmesstechnik.* lecture notes, 2003.

[19] Mangan, B. J., L. Farr, A. Langford, P. J. Roberts, D. P. Williams, F. Couny, M. Lawman, M. Mason, S. Coupland, R. Flea, H. Sabert, T. A. Birks, J. C. Knight . P. S. Russell: *Low loss (1.7 dB/km) hollow core photonic bandgap fiber*, 2004.

[20] Meyerand, R. G. . A. F. haught: *Gas breakdown at optical frequencies.* Physical Review Letters, 11(9):401–403, nov 1963.

[21] Mitschke, F.: *Glasfasern - Physik und Teschnologie.* Elsevier, 1 ., 2005.

[22] Plihal, M. . A. A. Maradudin: *Photonic band structure of two-dimensional systems: The triangular lattice*. Physical Review B, 44(16):8565–8571, oct 1991.

[23] Prechtl, A.: *Theoretische Elektrotechnik*. lecture notes, 1998.

[24] Reider, G. A.: *Photonik - Eine Einführung in die Grundlagen*. Springer-Verlag, 2 ., 1997.

[25] Russell, P. S.: *Photonic Crystal Fibers*. Science, 299:358–362, January 2003.

[26] Russell, P. S.: *Photonics*. lecture notes, 2004.

[27] Sasnett, M. W.: *Laser Beam Diagnostics*, jan 1991.

[28] Shephard, J. D., J. D. C. Jones, D. P. Hand, G. Bouwmans, J. C. Knight, P. S. Russell . B. J. Mangan: *High energy nanosecond laser pulses delivered single-mode through hollow-core PBG fibers*. Optics Express, 12(4):717–723, feb 2004.

[29] Siegman, A. E.: *Optical Resonators*, jan 1990.

[30] Stakhiv, A.: *Propagation of laser pulses through modern hollow fibers*. master thesis, 2003.

[31] Stuart, B. C., M. D. Feit, S. Herman, A. M. Rubenchik, B. W. Shore . M. D. Perry: *Nanosecond-to-femtosecond laser-induced breakdown in dielectrics*. Physical Review B, 53(4):1749–1761, jan 1996.

[32] Wintner, E.: *Laser in der Medizintechnik*. lecture notes, 2005.

[33] Wolfsberger, K.: *Theoretische Analyse von optischen Lichtwellenleitern als Filter transversaler Moden*. master thesis, 2003.

[34] Zhu, Z. . T. G. Brown: *Analysis of space filling modes of photonic crystal fibers*. Optics Express, 8(10):547–554, may 2001.

[35] Zoppel, S., R. Merz, J. Zehetner . G. A. Reider: *Enhancement of laser ablation yield by two color excitation*. Applied Physics A, 81:847–850, may 2005.

Appendix A.

Logarithmic Units

Logarithmic units are used to display the ratio of two physical values. Especially amplitude and power values are given in comparison. The values are based on decade or natural logarithm. The most common case is the use of the decade logarithm. The unit is called then "Bel [B]" or "Decibel [dB]". Generally, attenuation (a), gain (g) and ratio of output power versus input power (η) are declared. For the case of attenuation (a) some examples are mentioned.

Amplitude (A):

$$a_{\mathrm{B}} = 2 \lg_{10} \frac{A_1}{A_2}. \tag{A.1}$$

$$a_{\mathrm{dB}} = 20 \lg_{10} \frac{A_1}{A_2}. \tag{A.2}$$

Usually the power (P) is given as the square of the Amplitude, A^2. This means for power:

$$a_{\mathrm{B}} = \lg_{10} \frac{P_1}{P_2} = \lg_{10} \frac{(A_1)^2}{(A_2)^2} = \lg_{10} \left(\frac{A_1}{A_2} \right)^2 = 2 \lg_{10} \frac{A_1}{A_2}. \tag{A.3}$$

$$a_{\mathrm{dB}} = 10 \lg_{10} \frac{P_1}{P_2} = 10 \lg_{10} \frac{(A_1)^2}{(A_2)^2} = 10 \lg_{10} \left(\frac{A_1}{A_2} \right)^2 = 20 \lg_{10} \frac{A_1}{A_2}. \tag{A.4}$$

For the sake of completeness, some practical aspects are denoted. 50 % loss of power means a loss of 3 dB (or ratio of -3 dB),

$$a_{\mathrm{dB}} = 10 \lg_{10} \frac{\frac{1}{2}P_1}{P_1} = 10 \lg_{10} \frac{1}{2} = -10 \cdot 0.30103 = -3. \tag{A.5}$$

In the case of the PBG fiber the attenuation is specified to 60 dB/km or 0.06 dB/m. This indicates that using 1 km of fiber causes attenuation of 1,000.000 to the incident power or in other words every 50 meters the half of the power is lost.

$$\begin{aligned} 60 &= 10 \lg_{10} \frac{P_{in}}{P_{out}}, \\ 6 &= \lg_{10} \frac{P_{in}}{P_{out}}, \\ 10^6 &= \frac{P_{in}}{P_{out}}, \\ 10^6 P_{out} &= P_{in}. \end{aligned}$$

Appendix B.

Calculation of the focal distance of a thin lens

Following formulas are in use:

$$w_0\Theta = M^2\frac{\lambda}{\pi} \tag{B.1}$$

denoting the parametric beam product including the waist (w_0), divergence (Θ), wavelength (λ) and optionally M^2. Next, NA denotes the numerical aperture of the focusing or collimating lens and gives the following relation,

$$NA = \sin\Theta \approx \Theta. \tag{B.2}$$

$$\Theta = \frac{d_l}{2f} \tag{B.3}$$

where d_l denotes the lens aperture and f the focal distance, which leads to

$$w_0\frac{d_l}{2f} = M^2\frac{\lambda}{\pi} \tag{B.4}$$

$$w_0 = M^2\frac{2f\lambda}{d_l\pi} \tag{B.5}$$

and with

$$d_f = 2w_0 \tag{B.6}$$

one gets the focal spot diameter (d_f)

$$d_f = M^2\frac{2f\lambda}{d_l\pi}. \tag{B.7}$$

or with given (or desired) focal spot diameter, one can calculate the focal length with

$$f = \frac{\pi d_l d_f}{2\lambda M^2} \tag{B.8}$$

For the focal distance of the simple lense, we get for the laser "Quantel Brilliant"

$$\lambda = 1.064 \mu m$$

$$d_{beam} = d_l = 5.6 mm$$

$$M^2 = 1.42$$

With the equation B.8 one gets for the focal distance

$$f = \frac{\pi \cdot 5.6 mm \cdot 10 \mu m}{2 \cdot 1.064 \mu m \cdot 1.42}$$

$$f = 5.82208\, cm$$

With simple lense with the focal length of $f = 7.5 mm$, and the equation (B.7) one achieves a focal spot diameter of

$$d_f = 1.42 \cdot \frac{2 \cdot 7.5 mm \cdot 1.064 \mu m}{5.6 mm \cdot \pi}$$

$$d_f = 1.2882\, \mu m.$$

The calculation assumes ideal properties of the lens and the laser beam.

Appendix C.

Energy, power and intensity calculations

There are some essential relations between energy (E), power (P) and intensity (I). The conversion of energy to power:

$$P = \frac{E}{t} \tag{C.1}$$

where t denotes time duration (e.g. laser pulse duration).

Intensity can be calculated as follows:

$$I = \frac{P}{A} = \frac{\frac{E}{t}}{A} \tag{C.2}$$

where A indicates a cross sectional area.

As an example the peak power and intensity of a laser pulse are calculated,

Laser pulse duration, $\tau_p = 5\ ns$
Initial energy of the pulse, $E_p = 100\ \mu$J
Diameter of the spot, $d_{spot} = 15\ \mu$m

$$P_{peak} = \frac{E_p}{\tau_p} = \frac{100 \cdot 10^{-6}}{5 \cdot 10^{-9}} = 20 \cdot 10^3 = 20\, kW$$

$$I = \frac{P_{peak}}{A} = \frac{20 \cdot 10^3}{\pi \cdot (7.5)^2 \cdot 10^{-12}} = 0.113 \cdot 10^{15} = 113\, TW/m^2 = 11.3177\, GW/cm^2.$$

For plasma formation in the air, intensity of approximately 180 GW/cm^2 is needed or 15.9 times the pulse energy of 100 μJ is required, namely 1.59 mJ.